A Novel Framework of Multi-Hop Wireless Charging for Sensor Networks Using Resonant Repeaters

Cong Wang, Ji Li, Fan Ye, and Yuanyuan Yang, *Fellow, IEEE*

Abstract—Wireless charging has provided a convenient alternative to renew nodes' energy in wireless sensor networks. Due to physical limitations, previous works have only considered recharging a single node at a time, which has limited efficiency and scalability. Recent advances on multi-hop wireless charging is gaining momentum and provides fundamental support to address this problem. However, existing single-node charging designs do not consider and cannot take advantage of such opportunities. In this paper, we propose a new framework to enable multi-hop wireless charging using resonant repeaters. First, we present a realistic model that accounts for detailed physical factors to calculate charging efficiencies. Second, to achieve balance between energy efficiency and data latency, we propose a hybrid data gathering strategy that combines static and mobile data gathering to overcome their respective drawbacks and provide theoretical analysis. Then, we formulate multi-hop recharge schedule into a bi-objective NP-hard optimization problem. We propose a two-step approximation algorithm that first finds the minimum charging cost and then calculates the charging vehicles' moving costs with bounded approximation ratios. Finally, upon discovering more room to reduce the total system cost, we develop a post-optimization algorithm that iteratively adds more stopping locations for charging vehicles to further improve the results while ensuring none of the nodes will deplete battery energy. Our extensive simulations show that the proposed algorithms can handle dynamic energy demands effectively, and can cover at least three times of nodes and reduce service interruption time by an order of magnitude compared to the single-node charging scheme.

Index Terms—Wireless sensor networks, multi-hop wireless charging, resonant repeater, mobile energy replenishment, mobile data gathering, hybrid data gathering

1 Introduction

Wireless power transfer has been recently exploited in battery-powered wireless sensor networks (WSNs) to extend network lifetime towards perpetual operations. For high charging efficiency, charging vehicles (denoted as "SenCars" henceforth) are employed to approach sensor nodes in close proximity [1], [2], [3], [4], [11], [15], [36] and we refer to this type of networks as *wireless rechargeable sensor networks* (WRSNs). However, because the charging efficiency decays as an inverse cube of distance, most of the previous works only considered "short-range" charging where a SenCar needs to approach nodes in very close proximity and can only recharge the nodes one by one. This may lead to extremely long recharging latency: If a rechargeable battery takes 1–4 hours to fully recharge, a network of hundreds of nodes can take days or weeks. During such long latencies some nodes may exhaust energy and cause service interruption.

Inspired by the latest advances in mid-range wireless charging (where mid-range refers to energy transmitting distances much larger than the diameter of coils) that can relay energy over several hops to simultaneously replenish multiple nodes, in this paper, we explore how to leverage this technology to solve the above problems and enhance network scalability and performance.

One of the most cost-effective means to relay energy is to use *resonant repeaters*. Resonant repeaters can be easily manufactured from copper coils at low costs. In [13], significant improvements (10–46 percent) in efficiency are reported by adding resonant repeaters between the source and receiving coils. In [14], distributing 15 mW energy over a distance of 2 m to 6 different loads through 4 resonant repeaters has been demonstrated (Fig. 1a). In [16], experiments have shown that resonant repeaters can be organized into a domino form to power a 14W lamp (Fig. 1b). Their theoretical results indicate up to 50-70 percent charging efficiency even after 5–6 hops of relays.

For WRSNs, only very few works have considered recharging nodes in multi-hops [8], [9]. Although pioneering first steps, these works do not consider the physics laws governing wireless charging efficiency. In practice, the efficiency is not only impacted by the distance and vehicle's position, but also by a series of phenomenons such as cross-coupling where complex interactions between neighboring resonant repeaters cannot be simply ignored. Further, unlike data flows whose rates can be continuously adjusted, an energy flow can be turned on/off but there is no easy means to alter its rate over links [16]. Thus these works would deviate from real network operating conditions.

• *The authors are with the Department of Electrical and Computer Engineering, Stony Brook University, Stony Brook, NY 11794.*
E-mail: {cong.wang, ji.li, fan.ye, yuanyuan.yang}@stonybrook.edu.

Manuscript received 15 May 2015; revised 2 May 2016; accepted 6 May 2016. Date of publication 12 May 2016; date of current version 2 Feb. 2017.
For information on obtaining reprints of this article, please send e-mail to: reprints@ieee.org, and reference the Digital Object Identifier below.
Digital Object Identifier no. 10.1109/TMC.2016.2567382

(a) Distribute 15mW energy to 6 loads by 4 repeaters over 2m. Repeater coils are twisted on the black wheels with loads separated in between (courtesy of [14]).

(b) Power a 14W lamp by organizing repeaters into domino form (courtesy of [16]).

Fig. 1. Experimental prototypes of multi-hop wireless charging using resonant repeaters[14], [16]. (a) Distribute 15mW energy to 6 loads by 4 repeaters over 2 m. Repeater coils are twisted on the black wheels with loads separated in between (courtesy of [14]). (b) Power a 14W lamp by organizing repeaters into domino form (courtesy of [16]).

To tackle these limitations, in this paper we propose a new multi-hop wireless charging framework to improve charging capability and scalability. With a low-cost repeating circuit installed, sensor nodes can relay energy to their neighbors. Since previous single-node recharge scheduling algorithms do not consider such energy relaying, we provide a new recharge scheduling algorithm for this fundamentally different charging model. Furthermore, energy replenishment has to be considered together with energy consumption patterns, which depend largely on how data are collected. Mobile data gathering reduces energy consumption on intermediate nodes but incurs extra delivery latency [6], [7], [10], [11], [12], [37], [38] whereas static data gathering has shorter latency but much higher energy costs on routing paths [3]. To achieve a reasonable balance between latency and energy consumption, we introduce a *hybrid data gathering* strategy, where *time-sensitive* data are directly forwarded to the base station and *time-insensitive* data are gathered by mobile collectors.

The new framework raises several interesting questions. First, how to quantify the improvements from charging capability compared to the single-node recharge in terms of the number of nodes a SenCar can cover, and the number of SenCars needed? Second, given time-varying recharge requests, where SenCars should stop to recharge surrounding nodes such that multi-hop wireless charging cost is minimized and how to schedule the SenCars to minimize the moving cost? Third, are there any relationships between the two types of costs and is there a way to minimize the total system cost? Finally, what is the tradeoff among energy efficiency, network scalability and packet latency compared to the single-node recharge scheme?

To answer these questions, we first show how to accurately calculate wireless charging efficiency based on well-established methods in physics and electronics [16], so as to estimate energy charging cost during multi-hop relay. Then we theoretically analyze the energy consumptions under the hybrid data gathering model and estimate the improvements of using multi-hop charging. Based on the mathematical model, we can derive the number of SenCars needed to cover a network. Further, to minimize both charging and moving costs, we formulate recharge scheduling into a problem in the category of location-routing problems [20] with two objectives. Since the problem is NP-hard, we propose a two-step approximation algorithm that guarantees all energy demands are satisfied while minimizing the costs. In the first step, we identify a set of representative sensor locations (called "anchors") where SenCars stop and recharge nearby nodes such that overall charging cost is minimized. Our algorithm achieves a bounded approximation ratio of $\log n$ to the optimal solution (where n is number of nodes). In the second step, we first utilize an approximation algorithm for the Traveling Salesmen Problem to compute a complete shortest recharge tour through anchors. Then we assign recharge routes for different SenCars by dividing the complete tour according to SenCars' recharge capacity, energy demands and multi-hop charging cost. Given the selection of anchors, our algorithm generates recharge tours with the moving cost on SenCars bounded by $(\frac{5}{2} - \frac{1}{2k})$ ratio to the optimal result (where k is number of tours). Finally, upon discovering more room exists to optimize the system cost (charging cost plus moving cost), we propose a post-optimization algorithm that iteratively changes nodes with low charging efficiency into anchors and inserts them back into the established routes to further reduce the overall system cost.

We summarize the contributions of this paper as follows. First, we adopt resonant repeaters to improve charging capability based on realistic modeling of charging efficiency under physics laws. Second, we introduce a hybrid data gathering strategy to achieve balance between routing cost and data latency, and theoretically study scalability improvements. Third, we formulate recharge scheduling into a bi-objective optimization problem and propose a two-step approximation algorithm with bounded approximation ratios for each objective. We discover subtle relations between cost objectives and propose a post-optimization approach to further reduce the system cost while retaining nodes' battery deadlines. Our evaluation shows that the post-optimization algorithm can reduce the system cost by an additional 25 percent and the proposed framework can cover more than three times of nodes and has significantly less service interruptions compared to previous works. We also demonstrate trade-offs between multi-hop and single-node recharging methods, and relations between different optimization objectives. To the best of our knowledge, this is the first work on multi-hop wireless charging for WRSNs based on realistic physics models.

The rest of the paper is organized as follows. Section 2 presents a brief review on the previous works. Section 3 outlines the network model, and briefly describes how to compute charging efficiencies. Section 4 provides theoretical analysis of the framework. Section 5 formalizes multi-hop recharge scheduling into a bi-objective optimization problem and proposes a two-step approximation algorithm with a post-optimization algorithm given in Section 6. Section 7 provides simulation results. Finally, Section 8 gives some discussions and Section 9 concludes the paper.

2 Related Works

2.1 Single-Node Wireless Charging

Due to physical limits, most of the previous works consider "short-range" wireless charging that only a single sensor node is recharged each time. In [1], the impact of wireless charging on current designs of routing and deployment is studied. In [2], a greedy algorithm is designed to find a recharge sequence that maximizes network lifetime using mobile chargers. In [3], an optimization problem is studied to maximize the ratio between charging vehicle's idling and working time. In [4], a framework that dispatches and coordinates vehicles based on real-time energy status information is

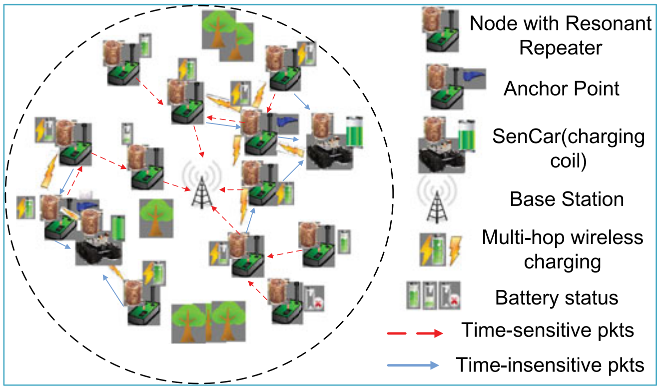

Fig. 2. Multi-hop wireless charging based on resonant repeaters.

proposed to achieve perpetual network operations. However, the optimization techniques and charging algorithms proposed in these works are based on single-node charging model which has very limited scalability. In addition, it is worth mentioning that our previous work [4] mainly focuses on the energy replenishment problem whereas energy consumptions due to communications are not considered. In this paper, besides multi-hop energy replenishment, we provide a comprehensive treatment for the energy consumption models based on the hybrid data gathering strategy.

2.2 Multi-Hop Wireless Charging

Multi-hop wireless charging for WRSNs is envisioned in [5], [8], [9]. In [5], a theoretical multi-hop charging model is proposed and the calculation shows that over 50 percent charging efficiency can be achieved for 4-5 hops of energy relays. However, how to utilize this technique to improve charging capabilities for WRSNs is not discussed. In [8], multi-hop wireless charging is formulated into energy flow problems that mimic data flow in the network. In [9], nodes in a network are organized into hexagonal cells and a SenCar stops at the cell center to recharge all the nodes. These works only focus on how to optimize multi-hop charging whereas leaving a gap between the solutions and fundamental physics. In this paper, we propose a new and comprehensive framework to bridge this gap by taking multi-hop charging efficiency into account.

3 Preliminaries

In this section, we introduce the network model and briefly describe the procedures to calculate multi-hop charging efficiency while taking comprehensive factors such as mutual inductance and cross-coupling into consideration.

3.1 Network Model

3.1.1 Network Components

Fig. 2 shows the basic components in our framework. We assume N static sensor nodes are uniformly randomly distributed in a circular field with radius R_c and node density $\rho = \frac{N}{\pi R_c^2}$. An embedded resonant repeater is added into the charging circuitry on both SenCars and sensors. It can be manufactured at low costs using copper wires/coils. For example, a 60 ft (18 m) copper tube is normally quoted for \$30-35[18], which is enough to make a dozen repeaters (average \$3-5 additional cost per node). Compared to the cost of a sensor node, which normally ranges from \$30-100, the increase of cost is about 10 percent.

In contrast to previous works in [8], [9], which do not provide any model of energy relay or charging efficiency, our framework establishes on physical models and provides concrete details by considering mutual inductance and cross-coupling effects between neighboring sensor coils. For simplicity, we assume all the nodes and SenCars have identical coils with n_t rounds and r_s radius. To successfully relay energy, nodes need to tune their resonant frequencies to the same frequency as SenCars and these nodes form a *charging set* around the stopping location of a SenCar. In practice, this is done by having different resonant frequency bands for neighboring charging sets. The band between different frequencies is wide enough to avoid any interference. Each sensor has a Ni-MH AAA battery with C_b capacity and its recharge time follows the data sheets in [19] (recharge time $T_r = 78$ mins).

To provide an effective charge that can stimulate enough currents on sensors' reception circuits, the charging efficiency η should be greater than a threshold τ, e.g., $\tau = 30\%$; otherwise, the node cannot be properly charged and it stops relaying wireless energy. We assume a charge controller is built into the circuit. It regulates the charging current to be a constant and stable value in order to protect the battery and elongate its lifespan.

3.1.2 Energy Consumptions

We consider multi-task sensing applications that sensors not only report *time-insensitive* data samples (e.g., temperature and humidity) from the environment periodically, but also detect N_e random events (e.g., lightening strike and tornado warning) that are *time-sensitive*. In a time slot, an event appears independently randomly from other events at a location. With sensing range R_s, an event is detected with probability $p = \frac{R_s^2}{R_c^2}$ for the node and its associated data rate is λ_1. Possible overlaps between nodes' sensing ranges may lead to redundancies in generated packets. To reduce sensing noises and estimation errors, it is desirable to preserve such redundancies so as to improve sensing robustness.

For *time-insensitive* data packets, we assume that data generation follows a constant bit rate of λ_2 because sensors are triggered periodically to gather environmental data.

The energy consumed for transmitting/receiving a packet of length l_p, denoted by e_c, is modeled as in [30], i.e., $e_c = (e_1 d_r^\alpha + e_0) l_p$, where d_r is the transmission range, e_1 is the loss coefficient per bit, α is the path loss exponent (usually from 2 to 4) and e_0 is the energy consumed on sensing, coding and modulations. A hybrid data gathering strategy is used in our framework to achieve a balance between packet latency and energy consumption. The *time-sensitive* data packets (with rate λ_1) due to event detection are directly forwarded towards the *base station* over multiple hops, while *time-insensitive* data packets (with rate λ_2) are gathered by SenCars during recharge to reduce routing cost. A latency upper bound for time-insensitive packets will be derived in the next section.

3.1.3 Energy Replenishment

If a node's battery level falls below threshold β, a recharge request is triggered and sent to SenCars. m SenCars respond

TABLE 1
List of Notations

Notation	Definition
N	Number of sensors
R_c	Radius of sensing field
R_s	Sensing range of sensors
N_e	Number of random events
λ_1, λ_2	Data rate of time-sensitive, time-insensitive packets respectively
d_r	Transmission range of sensor nodes
e_c	Energy consumption for transmitting/receiving a packet
m	Number of SenCars
C_b, C_h	Battery capacity of sensor nodes and SenCars, respectively
T_r	Recharge time of sensor's battery from zero to full capacity

to recharge requests cooperatively. Each SenCar is equipped with a relatively powerful high-capacity battery pack of capacity C_h and consumes e_s J/m energy while moving. SenCars stop at selected sensor locations (called *anchors*) to recharge nodes that have also requested for recharge with multi-hop energy relay and simultaneously gather data packets within l communication hops. If a node is within l-hops of SenCars, it always sends data to the closest SenCar to save energy on intermediate nodes.

To maintain perpetual operation of the network, the SenCars need to make every effort to recharge nodes before their battery energy depletes. For a recharge schedule, we denote the time instance when the SenCar begins to recharge sensor i (via multi-hops) by A_i. Then for the node with lifetime L_i, the SenCar should arrive before the battery depletes, $A_i \leq L_i$. $L_i = E_i/\mu_i$ where E_i is the residual battery energy and μ_i is the average traffic rates including the traffic relayed by i. In practice, it is common that the energy requests come in the form of bursts and the SenCars cannot handle all the requests at once. Some nodes that cannot be recharged on time will deplete energy and become nonfunctional temporarily. To this end, we introduce a term of *recharge delay*, q_i, to measure how long a SenCar misses the battery deadline of a node (late arrival). q_i takes the maximum value of $A_i - L_i$ and 0. That is, if $A_i > L_i$, a late arrival occurs and $q_i = A_i - L_i$; otherwise, $q_i = 0$. The recharge delay is also a measure of the time duration while a node is in nonfunctional status.

In addition, we make the following assumptions: 1) We assume the network is connected so messages can be exchanged among nodes. 2) Because nodes are static, network topology can be obtained at the initialization stage by a one-time effort. 3) To increase life cycles of batteries, only nodes in the charging range with energy below a threshold β will be recharged. Otherwise, they serve as energy relays for other nodes by switching on the resonant repeating circuit. 4) When the SenCar is about to deplete its battery, it goes back to the base station for a quick battery replacement. Finally, important notations are summarized in Table 1.

3.2 Multi-Hop Wireless Charging Efficiency

Calculating multi-hop wireless charging efficiency is the key in our framework. In this section, we describe an approach to estimate efficiency η_n after n relays. In principle, efficiency is governed by *mutual inductance*. Let L_{ij} denote the mutual inductance between repeaters on nodes i and j. From [17] we have

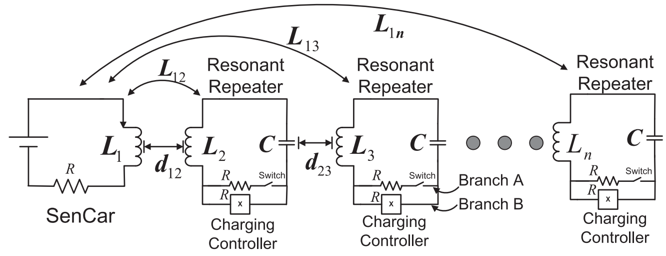

Fig. 3. A schematic of multi-hop wireless charging circuitries.

$$L_{ij} = \kappa_{ij}(n_t L_s)^2 \approx \frac{r_s^3}{2d_{ij}^3}(n_t L_s)^2, \quad (1)$$

where r_s is the coil radius, n_t is the number of rounds of coil wires, κ_{ij} is the magnetic *coupling coefficient* between nodes i and j ($0 \leq \kappa_{ij} \leq 1$), and L_s is the self-inductance of coils. $L_s = \mu_0 r_s(\ln \frac{8r_s}{r_d} - 2)$, r_d is the wire radius and μ_0 is the permeability constant equal to $4\pi \times 10^{-7} H \cdot \text{m}^{-1}$ (Henry per meter). The approximation is taken when wireless charging distance d_{ij} between i and j is much larger than the dimensions of coil radius r_s. Based on Kirchoff's Voltage Law, an established method in [16] can be used to calculate charging efficiency. The input voltage from SenCar's transmitting coil induces currents I_2-I_n on all sensor coils oscillating at frequency w and these values can be obtained by solving n linear equations as shown below (where $X = wL_s - \frac{1}{wC}$ and C is the capacitance).

$$\begin{pmatrix} R + jX & \cdots & jwL_{1n} \\ jwL_{12} & \cdots & jwL_{2n} \\ \vdots & \ddots & \vdots \\ jwL_{1(n-1)} & \cdots & jwL_{(n-1)n} \\ jwL_{1n} & \cdots & R + jX \end{pmatrix} \begin{pmatrix} I_1 \\ I_2 \\ \vdots \\ I_{n-1} \\ I_n \end{pmatrix} = \begin{pmatrix} V_{sc} \\ 0 \\ \vdots \\ 0 \\ 0 \end{pmatrix}$$

The above computation ensures that mutual inductance and cross coupling effects are accounted in our model. To maximize the utility of resonant repeaters, nodes finish charging their batteries should still act as energy relays. Denote the resistance of the charging circuit of branch B by R in Fig. 3. A resistor of the same R is added to match its resistance with the charging circuit. When a node is charging, switch at branch A is open and the output load is R. Once charging is finished, the battery stops charging and makes branch B open. Then we close the switch at branch A so the output load is still R. In this way, the charging efficiencies can stay the same despite some nodes might finish recharging earlier.

Although there are some energy cost in the repeating circuity, it can be justified from the following two aspects. First, since battery has a low internal resistance[19], the energy dissipated on the resistor for the given charging current is very small. Our model will successfully capture this factor into the calculations of charging efficiency next. Second, since nodes within SenCar's charging range share similar amounts of traffic load, the standard deviation of recharge times is small. Nodes within the same charging set usually finish charging at around the same time, thereby reducing the energy costs during these time gaps.

TABLE 2
Charging Efficiency versus Relay Hops

hops	1	2	3	4
$d = 0.25$ m	0.93	0.88	0.85	0.81
$d = 0.5$ m	0.89	0.68	0.54	0.39
$d = 0.75$ m	0.82	0.48	0.43	0.11
$d = 1$ m	0.78	0.33	0.27	0.03
$d = 1.25$ m	0.53	0.21	0.11	0.01
$d = 1.5$ m	0.35	0.08	0	0

While relaying energy, power consumption of the resonant repeater is the energy dissipated at the resistor R (i.e., $I_k^2 R$, where I_k is the constant current at branch of the k-th relay). The efficiency at the nth repeater output is

$$\eta_n = (RI_n^2)\Bigg/\left(R\sum_{k=1}^{n} I_k^2\right) = I_n^2\Bigg/\sum_{k=1}^{n} I_k^2. \tag{2}$$

As an example, in Table 2, we calculate the charging efficiency for up to 4 hops with $n_t = 300$ rounds and $r_s = 10$ cm coil radius while changing the hop-to-hop distance d from 0.25 to 1.5 m. First, we can see wireless charging efficiency decreases with more hops. This matches the intuition that energy relay attenuates rapidly from the source. Second, we observe that the efficiency decreases sharply when d is larger. This is because that the mutual inductance declines as an inverse cube of distance. For instance, when $d = 0.25$ m, charging efficiency after 4 hop relay (η_4) is still 81 percent. When $d = 1.5$ m, η_2 has reduced to 8 percent and hardly provides any effective charge for sensor's battery. Thus, the efficiency depends on the number of intermediate nodes that are relaying energy as well as the distance between them. Based on this method, each node can calculate energy cost during multi-hop charging by acting as a source where the SenCar might be residing at. Since the charging range is usually much less than the communication range, nodes can propagate requesting packets to know the positions of their neighbors and use this information to calculate charging efficiency.

4 Theoretical Analysis of Scalability

In this section, we theoretically analyze scalability improvements using resonant repeaters and calculate the number of SenCars required to achieve energy balance in the network.

4.1 Energy Consumptions

First, we analyze the energy consumption for hybrid data gathering which has two types of data destined either for the base station or SenCars. Denote the energy consumed in the network by these two types of data as E_b and E_s, respectively. The total energy consumption E in the network for a time slot is $E = E_b + E_s$. To obtain E_b and E_s, we need to first calculate the traffic destined for the base station (λ_1) and SenCars (λ_2). In each time slot, denote the probability that there is at least one event (among the total N_e events) in a node's sensing range as p_d. We have

$$p_d = 1 - (1-p)^{N_e} = 1 - \left(1 - \frac{R_s^2}{R_c^2}\right)^{N_e}. \tag{3}$$

Because time-sensitive packets are generated after the observation of events with probability p_d, the average traffic rate for time-sensitive packets is $p_d\lambda_1$ and we are interested in the values of E_b and E_s.

We assume that the radio coverage has a circular shape with d_r transmission distance so that at most $h = \lceil \frac{R_c}{d_r} \rceil$ hops are required to reach the outmost boundary of the sensing circle. We divide the network into h concentric rings where the ith ring carries all the traffic load from its outer rings ($i+1$ to h). For the uniform distribution of nodes with density ρ, the number of nodes in the ith ring is, $N_i = (2i-1)d_r^2\pi\rho$. We can calculate the average traffic rate $\lambda^{(i)}$ of the ith ring

$$\begin{aligned}\lambda^{(i)} &= (N_i e_c + 2\sum_{j=i+1}^{h} N_j e_c)\lambda_1 p_d \\ &= (2h^2 - 2i^2 + 2i - 1)\lambda_1 p_d d_r^2 \pi\rho e_c.\end{aligned} \tag{4}$$

By the same token, we derive the mean of E_b by taking the sum of λ_i from the 1st to the hth rings

$$\overline{E_b} = \sum_{i=1}^{h}(2h^2 - 2i^2 + 2i - 1)\lambda_1 p_d d_r^2\pi\rho e_c = \left(\frac{4}{3}h^3 - \frac{1}{3}h\right)\lambda_1 p_d d_r^2 \pi\rho e_c. \tag{5}$$

For estimating E_s, although the actual moving trajectories of m SenCars are unknown and quite difficult to analyze, we can view the data gathering process as m moving circles with radius ld_r ($l < h$). The total energy consumption for l-hop mobile data gathering can be obtained by replacing h with l and $\lambda_1 p_d$ with λ_2 in Eq. (5), yielding $(\frac{4}{3}l^3 - \frac{1}{3}l)\lambda_2 d_r^2\pi\rho e_c$. The best scenario with mobile data gathering is that all the time-insensitive packets generated in a time slot are gathered using l-hop communications. Statistically, each SenCar gathers data from $(d_r l)^2\pi\rho$ nodes, thus we can calculate E_s as

$$E_s = \left(\frac{4}{3}l^3 - \frac{1}{3}l\right)\lambda_2 d_r^2 \pi\rho N/(d_r^2 l^2 \pi\rho) = \left(\frac{4l^2 - 1}{3l}\right)\lambda_2 N e_c. \tag{6}$$

By combining Eqs. (5) and (6), we obtain the mean of E as

$$\overline{E} = \frac{4h^2 - 1}{3h}\lambda_1 p_d N e_c + \frac{4l^2 - 1}{3l}\lambda_2 N e_c. \tag{7}$$

4.2 Energy Replenishment

Our next objective is to estimate the energy replenishment in a time slot, R_e. Since charging efficiency depends on the actual number of sensor nodes that can relay energy, the procedure requires to solve a set of linear equations whose closed form result is difficult to derive. To circumvent these difficulties, we estimate the maximum charging capabilities of SenCars instead.

Assume a maximum charging range $r_{\max} = f(\rho, \tau)$ which is a function of node density ρ and efficiency threshold τ. In long term, the SenCars move almost everywhere in the field to satisfy energy requests. Instead of deriving the percentage of nodes that send out energy requests each time, it is sufficient to consider the ideal situation for estimating SenCar's maximum charging capability. That is, all the nodes within r_{max} request for recharge so the maximum number of nodes the SenCar recharges in multi-hops is

$\pi r_{max}^2 \rho$. In the worst case, if there is no node beyond the immediate hop in range $r_{\max}$, the scheme reduces to the conventional single node recharge.

For each recharge, a SenCar replenishes $(1-\beta)C_b$ energy for each node so the total energy it can put back into the network is $C_b(1-\beta)\pi r_{\max}^2\rho$. If SenCars keep replenishing node's battery one after another without any idle time, the only time overhead is the moving time between anchor locations. Since anchors could be anywhere during operations, we use the diameter which is the longest distance in the field as an upper bound on the moving distance, then the longest moving time $T_l = 2R_c/v$, where v is the speed of a SenCar. Hence, we can write the collective recharging rates from m SenCars as

$$R_e = \frac{mC_b(1-\beta)\pi r_{\max}^2\rho}{(T_l+T_r)}. \tag{8}$$

We can see that multi-hop wireless charging provides a scalability gain to cover $\max(\pi r_{\max}^2\rho, 1)$ more nodes compared to the single node recharge scheme. For example, $r_{\max} = 3$ m and $\rho = 0.25$ nodes/m^2, on average, a SenCar can replenish 7 nodes simultaneously by spending T_r time, thus speeding up 7 times compared to the single node recharge. This shows that given the same number of SenCars, multi-hop charging enjoys much better scalability to support larger networks.

4.3 Minimum Number of SenCars

Once we have the expressions for energy consumption and replenishment, we can set up an energy balance for the network by letting $E \leq R$. This relation states that in each time slot, the amount of energy consumed by sensor nodes should be at least equally replenished back into the network by the SenCars. By considering Eq. (7) and Eq. (8),

$$m \geq \left(\frac{4h^2-1}{3h}\lambda_1 p_d + \frac{4l^2-1}{3l}\lambda_2\right)\frac{(T_l+T_r)R_c^2 e_c}{(1-\beta)C_b r_{max}^2}. \tag{9}$$

Remarks: Since the SenCar's battery capacity C_h is much larger than the sensor's battery C_b, it does not go back to the base station for battery replacement frequently. Time overhead for such battery replacement is minimal compared to recharging sensors' batteries so we do not consider C_h in the above calculations. It is interesting to see from Eq. (9) that using multi-hop wireless charging, for fixed field sizes, the number of SenCars no longer depends on the number of sensor nodes in the network. This property has created opportunities to add more nodes into the network without increasing the number of SenCars. In practice, driven by the decreasing manufacturing cost of sensor nodes, redundancies are usually preferred to provide robustness and extra coverage. Our analysis has shown that multi-hop wireless charging helps network administrators improve scalability without incurring higher manufacturing and human labor costs of implementing more charging vehicles like the cases in single node recharge [1], [2], [3], [4], [11], [15].

We now illustrate Eq. (9) through an example. First, let us set $d_r = R_s = 5$ m, $N_e = 5$ events, $R_c = 25$ m, $l = 2$, $e_c = 0.025J$, $\lambda = 3$ pkt/min, $T_r = 78$ mins, $C_b = 780$ mAh,

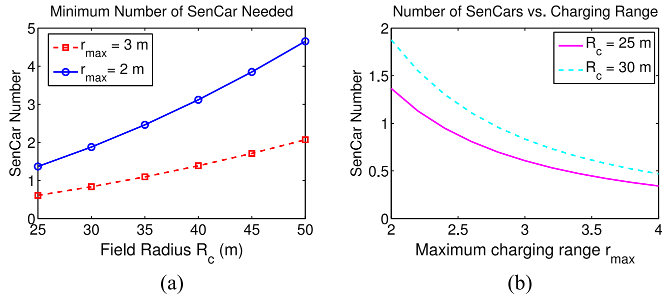

Fig. 4. Theoretical results for the number of SenCars. (a) Number of SenCars versus field sizes. (b) Number of SenCars versus maximum charging range.

$\beta = 50\%$, and $v = 1$ m/s. From Table 2 and simulations, an estimation of effective charging range for efficiency above 30 percent is $r_{\max} = 3$ m. By plugging these values into Eq. (9), we obtain $m \geq 0.61$, which means one SenCar can almost satisfy energy demands. For different charging range of 2 and 3 m, we examine the relations between the field size and the number of SenCars in Fig. 4a. We can see that the number of SenCars increases almost linearly with field size and a smaller charging range requires more SenCars to maintain energy balance. Similarly, we demonstrate the relation between the number of SenCars and charging range for different field sizes in Fig. 4b. We observe that as the charging range increases, the number of SenCars declines at a decreasing marginal rate.

4.4 Latency Bound for Time-Insensitive Packets

The hybrid data gathering framework ensures fast delivery of time-sensitive packets via multi-hop transmission. For energy saving, time-insensitive packets are collected by the SenCars and their latencies are subject to SenCars' mobility patterns. Since SenCars' mobility is random and difficult to analyze, in this section, we derive an upper bound for such latency. In our model, collected packets are buffered until the SenCar returns to the base station for battery replacement, the longest latency occurs when SenCar's battery is consumed at the slowest pace. It happens in the worse case that the SenCar can only recharge one node at a time and the sum of requested energy plus SenCar's moving energy is greater than or equal to SenCar's recharge capacity C_h. The time duration T_d to replenish all C_h energy into the network is bounded by

$$\begin{aligned} T_d &< \Big(C_h - \sum_{i=0}^{n-1} t_{i,i+1} v e_s\Big)/r_l + \sum_{i=0}^{n-1} t_{i,i+1} < \frac{C_h}{r_l} + \sum_{i=0}^{n-1} t_{i,i+1} \\ &< \frac{C_h T_r}{C_b(1-\beta)} + \frac{2R_c C_h}{C_b(1-\beta)v} = \frac{C_h(T_r v + 2R_c)}{C_b(1-\beta)v}, \end{aligned} \tag{10}$$

where r_l is the average recharging rate of the battery, n is the number of sensors in a tour and $t_{i,i+1}$ is the traveling time from nodes i to $i+1$ in the sequence. The relation holds because: 1) SenCar's moving energy in $\sum_{i=0}^{n-1} t_{i,i+1} v e_s$ is less than C_h and upper bounded by C_h; 2) $r_l \geq \frac{C_b(1-\beta)}{T_r}$. In other words, $\frac{C_b(1-\beta)}{T_r}$ is a lower bound for the charging rate since it takes less than T_r time to recharge the amount of $C_b(1-\beta)$ energy; 3) $n < C_h/(1-\beta)C_b$ (nodes will request for more than $(1-\beta)C_b$ energy) and $t_{i,i+1} \leq \frac{2R_c}{v}$ (diameter is the longest distance in the field). This numerical result will be evaluated through simulations in Section 7.6.

5 Scheduling SenCars for Multi-Hop Charging

In this section, we study how to schedule m SenCars for multi-hop wireless charging to respond to sensors' energy requests. A variety of practical factors, e.g., location-dependent charging efficiencies, energy charging cost, SenCar's recharge capacity, and energy consumption in movements, are brought into our problem formulation.

Our objectives are two-folds: on one hand, we aim to minimize the energy cost via multi-hop charging. It requires SenCars to select advantageous locations (anchors) for stopping so that overall charging efficiency is maximized. On the other hand, we want to minimize moving energy consumption for SenCars within their recharge capacities. In principle, our problem resembles the location-routing problem (LRP) [20]. LRP finds the optimal warehouse locations for minimum accessing and distributing costs of traversal routes over demand locations that start and end at warehouses. It encompasses two NP-hard problems, i.e., location and routing problems, and seeks to provide an integrated solution to optimize the overall system cost. However, instead of vehicles directly visiting each warehouse location in the original LRP, our problem involves an additional level of cover problem. That is, the anchors have to ensure that all sensors are "covered," i.e., be charged either directly or via multi-hops. Based on the energy requests at different times, SenCars need to calculate anchors and fulfill all requests from sensors adaptively.

Thus we formulate our problem in the context of LRP with two objectives that minimize both SenCars' charging cost and moving cost. Due to the NP-hardness nature of our problem, we propose a two-step approximation algorithm. In the first step, a ratio of $\log n$ to the optimal charging cost is achieved, where n is the total number of recharge requests. In the second step, given the selection of anchors, the maximum touring cost is bounded by a ratio of $(\frac{5}{2}-\frac{1}{2k})$ to the optimal solution, where k is the number of scheduled tours (normally, $k=m$). Finally, based on the results from the algorithm, we study the relationships between the two objectives and combine them into a single-objective problem using the weighted method [27]. A post-optimization algorithm is proposed to further reduce the total system cost by inserting anchors into the established routes.

5.1 Problem Formulation

We now present the formulation of our problem. During operations, energy information from sensor nodes can be gathered by SenCars using the methods in [4]. At time t, given the set of SenCars, $\mathcal{M}$, the set of sensor nodes requesting recharge, $\mathcal{N}$, the set of potential anchors where SenCars can stop, $\mathcal{A} (\mathcal{A} \subseteq \mathcal{N})$, and the set of starting locations of SenCars, $\mathcal{I}$, we formulate the problem as follows.

Consider a graph $G=(V,E)$, where V_i $(i \in \mathcal{N} \bigcup \mathcal{I})$ is the location of sensor node i, and E are edges connecting sensor nodes. The weight of an edge E_{ij} is the energy cost c_{ij} traveling on the edge, which is proportional to the distance between nodes i and j. Each SenCar has recharge capacity C_h corresponding to the maximum number of nodes and distance it can travel in each tour. A node i has energy demand d_i (which equals full capacity minus its residual energy). Each anchor a covers a set of nodes $\mathcal{S}_a$ and the entire covered set of all the anchors achieves $\mathcal{N}$ ($\bigcup \mathcal{S}_{a\in\mathcal{A}} = \mathcal{N}$). Recharging $\mathcal{S}_a$ requires t_a time which is usually determined by the node with the longest recharge time. For a node i, η_{ia} denotes the recharge efficiency when a SenCar resides at anchor a. Several decision variables are introduced in the formulation. x_{ijk} is 1 if anchor $i \in \mathcal{A}$ immediately precedes $j \in \mathcal{A}$ for SenCar k; otherwise, it is 0. For $i \in \mathcal{N}, k \in \mathcal{M}, a \in A$, y_{ia} is 1 if node i can be recharged when a SenCar resides at $a \in A$. z_{ik} is 1 if node i is recharged by SenCar k. u_a is 1 if an anchor a is chosen; otherwise, it is 0. v_{ik} is the position of anchor i in the path of SenCar k. Our objective is to minimize the charging cost in multi-hop energy relays, F_c, and SenCars' moving cost, F_m.

$$\textbf{P1}: \quad \min F = (F_c, F_m), \tag{11}$$

where,

$$F_c = \sum_{i\in\mathcal{N}} \sum_{a\in\mathcal{A}} \frac{1-\eta_{ia}}{\eta_{ia}} d_i y_{ia} \tag{12}$$

$$F_m = \sum_{i\in\mathcal{A}} \sum_{j\in\mathcal{A}} \sum_{k\in\mathcal{M}} c_{ij} x_{ijk} + \sum_{i\in\mathcal{I}} \sum_{j\in\mathcal{A}} \sum_{k\in\mathcal{M}} c_{ij} x_{ijk}, \tag{13}$$

Subject to

$$\sum_{i\in\mathcal{A}} x_{ijk} = z_{jk}, j \in \mathcal{A}, k \in \mathcal{M}, \tag{14}$$

$$\sum_{j\in\mathcal{A}} x_{ijk} = z_{ik}, i \in \mathcal{A}, k \in \mathcal{M}, \tag{15}$$

$$\sum_{a\in\mathcal{A}} y_{ia} = 1, i \in \mathcal{N}, \tag{16}$$

$$\eta_{ia} y_{ia} > \tau, i \in \mathcal{N}, a \in \mathcal{A}, \tag{17}$$

$$y_{ia} \leq u_a, i \in \mathcal{N}, a \in \mathcal{A}, \tag{18}$$

$$\begin{aligned} \sum_{i\in\mathcal{N}} z_{ik} \left(\sum_{a\in\mathcal{A}} d_i y_{ia}/\eta_{ia} \right) + \sum_{i\in\mathcal{A}} \sum_{j\in\mathcal{A}} c_{ij} x_{ijk} \\ + \sum_{i\in\mathcal{I}} \sum_{j\in\mathcal{A}} c_{ij} x_{ijk} \leq C_h, k \in \mathcal{M}, \end{aligned} \tag{19}$$

$$\sum_{k\in\mathcal{M}} z_{ak} = u_a, a \in \mathcal{A}, \tag{20}$$

$$2 \leq v_{ik} \leq |\mathcal{N}|, i \in \mathcal{A}, k \in \mathcal{M}, \tag{21}$$

$$\begin{aligned} & v_{ik} - v_{jk} + (|\mathcal{A}| - |\mathcal{M}|) x_{ijk} \leq |\mathcal{A}| - |\mathcal{M}| - 1 \\ & i, j \in \mathcal{A}, k \in \mathcal{M}, \end{aligned} \tag{22}$$

$$x_{ijk}, y_{ia}, z_{ik} \in \{0,1\}, i, j \in \mathcal{N}, a \in \mathcal{A}, k \in \mathcal{M}. \tag{23}$$

In the above formulation, constraint (14) and constraint (15) stipulate the connectivity of the path that a SenCar stopping at an anchor also leaves it. Constraint (16) imposes that all the nodes request recharge are covered by anchors. Constraint (17) ensures that the recharge efficiency for a node from its anchor should be larger than the efficiency threshold. Constraint (18) guarantees that a node is assigned to one of the anchors. Constraint (19) mandates that the sum of total demands serviced by a SenCar plus its moving energy consumptions should not exceed its recharge capacity. Constraint (20) enforces that each anchor is visited by only one SenCar. Constraints (21) and (22) are formed according to [21] to prevent subtours of SenCars. Constraint (23) forces x_{ijk}, y_{ia} and z_{ik} to be 0-1 valued.

Remarks: This formulation reflects recharge schedules at time t based on N energy requests (N is an input). For executions at different times, the optimization problem takes corresponding inputs and generates different results (anchors, SenCar schedules, etc). Although we do not formulate node lifetime strictly into the formulation, it will be considered by our algorithm in Sections 5.2.3 and 6.3.

The above problem is NP-hard because the location routing problem is known to be NP-hard [20]. Although standard optimization procedures can yield optimal solutions [20], it is prohibitive to run them on SenCars due to enormous computation overhead. The base station has computational resources. However, the communication overhead to maintain updated energy requests and disseminate recharge decisions for SenCars could be high in a long run. Moreover, the existing optimization methods are usually designed to handle static inputs and lack the flexibility to deal with constant variations in sensor networks such as battery energy and SenCar movements. Therefore, a polynomial-time approximation algorithm with an acceptable bounded ratio is more desirable in practice. To design the approximation algorithm, we follow a natural approach to tackling the objectives sequentially and finally examine the relationships between them. Next, we propose a two-step approximation algorithm which first selects the anchors that minimize energy charging cost, and then finds the minimum recharge routes for SenCars.

5.2 Approximation Algorithms

In this section, we explain the details of the algorithm. We first define a *charging set* $\mathcal{S}_i$ of node i as its nearby nodes with charging efficiencies larger than τ when a SenCar stops at node i. At the network initialization phase, each node performs the procedures in Section 3.2 to compute its charging set in a distributed manner. For node i, its neighbor j is included in $\mathcal{S}_i$ only if j's charging efficiency is larger than threshold τ and the corresponding efficiency is denoted as $\eta_{j,i}$ ($j \in \mathcal{S}_i$). The algorithm starts with finding the set of anchors based on the energy requests.

5.2.1 Adaptive Anchor Selection

We define the weight of each set $\mathcal{S}_i$ as the total energy needed to satisfy the recharge demands of these nodes, $w_i = \sum_{j\in\mathcal{S}_i}(1-\eta_{j,i})d_j/\eta_{j,i}$. It is not difficult to observe that our objectives in Eq. (12) is equivalent to minimizing the sum of weights of the selected sets. In general, this problem belongs to the category of *Set Cover Problem* (SCP) with one difference: While the original SCP allows the results to share the same nodes and thus resultant sets are not necessarily disjoint, our formulation restricts a node to be recharged by only one SenCar (Eq. (20)), since if a node can be recharged by more than one SenCars in different recharge routes, it is always preferred to assign the node to a charging set with higher charging efficiency. Hence in our problem, the resultant sets should be disjoint. Next, we modify the classic greedy approach to fit into the context of our problem.

Initially, we define sets $\mathcal{A}$ and $\mathcal{B}$ to record anchors and their covered node sets respectively and both sets are initialized to empty. First, for each node $i \in \mathcal{N}$, we compute its average weight, $\overline{w_i} = \sum_{j\in\mathcal{S}_i}\frac{(1-\eta_{j,i})d_j}{\eta_{j,i}}/|\mathcal{S}_i|$ and search for the set with the minimum $\overline{w_i}$. Assume node k's subset has the least average weight so k becomes an anchor. Then, it is added into $\mathcal{A}$ and $\mathcal{S}_k$ is put into $\mathcal{B}$ to be marked as "covered." In practice, this is done by tuning all the nodes in $\mathcal{S}_k$ to have the same resonant frequency (described in the next section). Since those nodes might be also covered by other sets, we need to remove them from the remaining sets. Their elements are updated accordingly, $\mathcal{S}_i = \mathcal{S}_i - B, \forall i\backslash k \in \mathcal{N}$. At this time, if $\mathcal{B}$ contains all the nodes in $\mathcal{N}$, the algorithm terminates. Otherwise, it continues to find the next set among the remaining nodes with minimum average weight until all the nodes are covered ($\mathcal{B} = \mathcal{N}$). Algorithm 1 shows the pseudo-code for the adaptive anchor selection algorithm.

Algorithm 1. Adaptive Anchor Selection Algorithm

Input: Recharging node set $\mathcal{N}$, charging set $\mathcal{S}_i$, energy demand d_i, charging efficiency of node j.
Output: Set of anchors $\mathcal{A}$ and resultant subsets $\mathcal{B}$.

```
1: while B ≠ N do
2:    Calculate w̄_i = Σ_{j∈S_i} (1−η_{j,i})d_j/η_{j,i} / |S_i|.
3:    Find minimum weight k = arg min_i w̄_i, i ∈ N.
4:    A ← A ⋃ k, B ← B ⋃ S_k, S_i ← S_i − B, ∀i\k ∈ N.
5: end while
```

5.2.2 Resonant Frequency Assignment

After the anchors have been found in the first step, we need to assign resonant frequencies in order to distinguish charging sets and avoid potential interference. By tuning to a proper frequency, nodes can "join" or "leave" a set very easily. Given an available resonating frequency range, we divide it into numerous frequency bands and each band should be reused as long as there is no interference between the neighboring charging sets, i.e., the frequency assignment for each charging set and its neighbors are different. This problem is equivalent to the classic vertex coloring problem [22] which tries to color nodes in a graph with as small number of colors as possible such that no two adjacent nodes have the same color. Here, the vertice are anchors and edges are connections represented by energy relays between anchors if the distance between any two elements in their charging sets is less than the maximum charging range $r_{\max}$. Unfortunately, vertex coloring is a well-known NP-hard problem and it even turns out that approximation within $n^{1-\epsilon}$ is NP-hard ($0 < \epsilon < 1$, $n = |\mathcal{A}|$) [23]. For a reasonable balance between computation complexity and optimality, we propose an algorithm that uses at most $\max_{1\le i\le|\mathcal{A}|}(\Delta_i + 1)$ frequency bands, where Δ_i is the degree of anchor i. A set of frequency bands is denoted by $\mathcal{F} = \{f_1, f_2, \ldots, f_n\}$.

After the anchors are determined in Section 5.2.1, the algorithm starts from an arbitrary anchor in $\mathcal{A}$ and uses f_1 as its resonant frequency. Then it proceeds to the next anchor and uses available frequency band with the lowest f_i if it is not used by any of its neighboring anchors. The algorithm terminates when all the anchors in $\mathcal{A}$ are assigned proper frequency bands. At this point, the anchors, charging sets and their resonant frequencies are determined and these decisions are disseminated to the anchors. Anchors also send out packets carrying their corresponding frequency information within the boundary of their charging sets. Since the maximum charging range $r_{\max}$ is usually less than transmission distance d_r, the construction of charging sets is done easily by one-hop transmission. Thus, the message overhead is $O(|\mathcal{N}-\mathcal{A}|)$. The algorithm is summarized in Algorithm 2.

Note that the upper bound of $\max_{1\le i\le|\mathcal{A}|}(\Delta_i+1)$ holds because an anchor i has at most Δ_i neighboring anchors and occupies at most Δ_i frequency bands (some of the neighboring anchors may have already been assigned frequencies). By the same token, for the anchor with the maximum degree, at most the same amount of frequency bands are needed for its neighbors. Thus, it is not difficult to see the upper bound holds at the maximum degree of anchors.

Algorithm 2. Resonant Frequency Assignment Algorithm

Input: Set of anchors $\mathcal{A}$, set of frequency bands $\mathcal{F}$.
Output: Frequency assignment f_a, $\forall a\in\mathcal{A}$.
1: Establish connections among anchors based on $r_{\max}$.
2: **while** $\mathcal{A}\neq\emptyset$ **do**
3: Check the frequency of anchor a's neighbors, denoted by $\mathcal{F}'$.
4: Find available frequency bands, $\mathcal{F}\leftarrow\mathcal{F}-\mathcal{F}'$.
5: Assign frequency $\min(f_k)$ $k\in\mathcal{F}$ to anchor a.
6: Set frequency of nodes in charging set $\mathcal{S}_a$ to f_k, $\mathcal{A}\leftarrow\mathcal{A}-a$.
7: **end while**

5.2.3 Schedule Recharge Routes

After the set of anchors $\mathcal{A}$ has been found, we assign the recharge routes for m SenCars while considering SenCars' capacities along with their moving cost and multi-hop charging cost. Based on [24], we propose an approximation algorithm to bound SenCars' moving energy cost given the anchors. Our approach first utilizes a Traveling Salesman Problem (TSP) algorithm to compute a complete route on $\mathcal{A}$, e.g., 1.5-approximation Christofides algorithm [25]. In this way, we can ensure that anchors close to each other are placed on the same SenCar's recharge route. To facilitate our analysis, we assume that the complete tour starts at the base station and ends at the last node for recharge. In fact, the starting positions of SenCars are the ending positions from the last tours and SenCars traverse through the base station to upload data packets. The recharge sequence can be expressed as $r=(b,1,2,\dots,i,\dots,n)$, where anchor $i\in\mathcal{A}, n=|\mathcal{A}|$ and b is the base station. To reflect SenCar's starting position, an extra edge with cost $c_{i,b}, i\in\mathcal{I}$, can be added to represent the energy cost from SenCar's starting location $i\in\mathcal{I}$ to the base station b. Let $c_{\max}$ denote the maximum energy cost from any node on the path to the base station, $c_{\max}=\max_{i\in\mathcal{A}\bigcup\mathcal{I}}c_{b,i}$. The TSP algorithm yields a complete route r that incurs c_r energy cost using one SenCar.

Next, r is split into k tours. For partitioning, we start with an arbitrary direction along r. For each route j, $1\le j\le k$, we find the last anchor along the complete tour r that ensures the traveling energy cost is no greater than $\frac{j}{k}(c_r-c_{\max})+2c_{\max}$. Here, the term $2c_{\max}$ is the maximum energy cost from SenCar's starting position to the base station plus the cost from the base station to the first anchor on the recharge path. Then r will be split into k tours. Let a_i^j and a_l^j represent the ith and the last nodes in the j-th tour, respectively. The j-th tour is then obtained as $(\mathcal{I}_j,b,a_1^j,a_2^j,\dots,a_l^j)$.

k depends on SenCars' recharge capacity (constraint in Eq. (19)). We check whether an equal division of m SenCars from the total energy cost is less than SenCar's capacity. Depending on the results, there are two cases:

Case 1: If an equal division of m among the total cost is less than SenCar's capacity C_h, $k=m$. In this case, m SenCars are sufficient to cover all the nodes in one shot.

Case 2: Otherwise, $k>m$ and,

$$k=\left\lceil\left(\sum_{i\in\mathcal{A}}\sum_{j\in\mathcal{S}_i}\frac{(1-\eta_{j,i})d_j}{\eta_{j,i}}+c_r-c_{\max}\right)\Big/(C_h-2c_{\max})\right\rceil. \quad (24)$$

This case usually occurs when the temporary energy demands overwhelmingly exceed SenCars' recharge capacity so that they have to take $\lceil\frac{k}{m}\rceil$ rounds to cover all the routes. In each round, at most m routes can be selected from k, thus late recharge for some nodes is inevitable. Therefore, our objective is to reduce the recharge delay as much as possible. Let us denote the recharge time for node i by t_i and traveling time between nodes i and $i+1$ by $t_{i,i+1}$ in the recharge sequence. For multi-hop wireless charging, the SenCar leaves an anchor after it has fulfilled all requests in a charging set, so the recharge time of $\mathcal{S}_a$ is $t_a=\max_{i\in\mathcal{S}_a}(t_i)$. The total time duration for a route j is $T_j=\sum_{a=1}^{l_j}t_a+\sum_{a=1}^{l_j-1}t_{a,a+1}$. The longest route takes the maximum time among T_j to finish. For route j, if it is selected by a SenCar in the current round, the recharge delay of all the nodes is

$$P_j=\sum_{i\in\bigcup\mathcal{S}_k^j,k\in\mathcal{A}^j}q_i=\sum_{i\in\bigcup\mathcal{S}_k^j,k\in\mathcal{A}^j}\max(A_i-L_i,0). \quad (25)$$

However, if route j is not selected, in the next round, the worst case occurs when it has to wait for the longest route to finish. Then the recharge delay is

$$P_j'=\sum_{i\in\bigcup\mathcal{S}_k^j,k\in\mathcal{A}^j}\max(A_i+T_{\max}-L_i,0). \quad (26)$$

An increment

$$\Delta P_j=\sum_{i\in\bigcup\mathcal{S}_k^j,k\in\mathcal{A}^j}\big(\max(A_i+T_{\max}-L_i,0)-\max(A_i-L_i,0)\big), \quad (27)$$

is observed. To keep recharge delay minimal, we sort ΔP_j and select the m routes with the largest increment in each round so that those routes that would incur longer delay can be recharged in the current round. The pseudo-code of the algorithm is presented in Algorithm 3.

Algorithm 3. Route Scheduling Algorithm

Input: Set of anchors $\mathcal{A}$, SenCars $\mathcal{M}$, energy demand d_i of node i, charging efficiency of node j, $\eta_{j,i}$ when SenCar is at i. Set of SenCars' initial locations $\mathcal{I}$, capacity C_h, base station b, max energy cost traveling on an edge $c_{\max}$.
Output: Recharge sequence r_j for SenCar j's tour.

if $(\sum_{i\in\mathcal{A}}\sum_{j\in\mathcal{S}_i}\frac{(1-\eta_{j,i})d_j}{\eta_{j,i}} + c_r - c_{\max})/m + 2c_{\max} < C_h$ **then**
  $k = m$,
else
  $k = \lceil(\sum_{i\in\mathcal{A}}\sum_{j\in\mathcal{S}_i}\frac{(1-\eta_{j,i})d_j}{\eta_{j,i}} + c_r - c_{\max})/(C_h - 2c_{\max})\rceil$.
end if
Start with an arbitrary direction on r, $j = 1$
while $r \neq \emptyset$ **do**
  For tour j, search for the last node a_l^j along r.
  Satisfying $c_j \leq \frac{j}{k}(c_r - c_{\max}) + 2c_{\max}$.
  Obtain the j-th tour, $(\mathcal{I}_j, b, a_1^j, a_2^j, \dots, a_{l_j}^j), 1 \leq j \leq k$.
  Exclude nodes in j-th tour from r. $j \leftarrow j + 1$.
end while
if $k = m$ **then**
  Assign each SenCar to a recharge route
else
  $T_{\max} = \max_{j=(1,2,\dots,k)}(\sum_{a=1}^{l_j} t_a + \sum_{a=1}^{l_j-1} t_{a,a+1})$,
  $\Delta P_j = \sum_{i\in\bigcup\mathcal{S}_k^j, k\in\mathcal{A}^j}\big(\max(A_i + T_{\max} - L_i, 0) - \max(A_i - L_i, 0)\big)$.
  Sort ΔP_j and select the m largest for recharge each round.
end if

5.3 Approximation Bounds and Complexity

We now analyze the approximation bounds for the proposed algorithm. For $n = |\mathcal{N}|$ recharge requests, our algorithm gives a $\log n$ approximation of the energy cost during multi-hop wireless charging and a $(\frac{5}{2} - \frac{1}{2k})$ ratio for the traveling cost given the selected anchors, where k is the number of tours depending on energy demands and recharge capacity C_h. In the extended greedy algorithm of the Set Cover Problem, we assume the optimal energy cost is w^*. During computation, when there are i nodes left to be covered, it incurs at most $\frac{w^*}{i}$ energy cost per node. The bound of the extended greedy algorithm is thus $\sum_{i=1}^{n}\frac{w^*}{i} = w^*\log n$. The equality holds because the summation $\sum_{i=1}^{n}\frac{1}{i} = \log n$ is the n-th harmonic number.

Remarks: Although the $\log n$ bound for energy charging cost seems quite large, it is essentially one of the best polynomial-time approximation algorithms: it has been proved in [26] that the Set Cover Problem cannot be approximated in polynomial time within a ratio of $c\log n$, for $c < \frac{1}{4}$, under general complexity assumptions. A tighter bound might not be necessary given the increased complexity and transient nature of energy requests.

Next, we show that the traveling energy cost has an approximation ratio of $(\frac{5}{2} - \frac{1}{2k})$ respect to k tours. Here, when $k > m$, the $k - m$ tours are traversed by SenCars after they have replaced batteries in the base station. Nevertheless, the total cost would still be the same. For the complete tour, the energy cost is c_r with the optimal value c_r^*. Use Christofide's minimum spanning tree approximation to the TSP, $\frac{c_r}{c_r^*} \leq 1.5$ [25]. Assume that tour j has the maximum energy cost c_j among k tours and its optimal value is c_j^*. The energy cost for tour j is at most $\frac{1}{k}(c_r - c_{\max})$ (excluding the edge leaving the base station in the complete tour r) plus $2c_{\max}$ for the two edges connecting the base station to SenCar's starting position and the first anchor in each tour. Therefore, $c_j \leq \frac{1}{k}(c_r - c_{\max}) + 2c_{\max} = \frac{1}{k}c_r + (2 - \frac{1}{k})c_{\max}$. We divide both sides by c_j^* and have

$$\frac{c_j}{c_j^*} = \frac{1}{k}\frac{c_r}{c_j^*} + \left(2 - \frac{1}{k}\right)\frac{c_{\max}}{c_j^*} \leq \frac{1}{k}k\frac{c_r}{c_r^*} + \left(2 - \frac{1}{k}\right)\frac{1}{2} \leq \frac{5}{2} - \frac{1}{2k}. \tag{28}$$

The inequality holds because for each tour, an edge is added to connect the first sensor node to the base station, $c_r^* \leq \sum_{i=1}^{k} c_i^*$. If we divide both sides by k and use the fact that $\max_{1\leq i\leq k}(c_i^*) = c_j^*$, we have $\frac{c_r^*}{k} \leq c_j^*$. We take the approximation $c_{\max} \leq \frac{1}{2}c_j^*$. The equality holds when the tour has only one node.

Let us denote the number of energy requests by N and the number of anchors by A. The time complexity of the anchor selection algorithm is $\mathcal{O}(N\log N)$ because if we first sort nodes according to their weights, $\mathcal{O}(N\log N)$ is required. In each step, we select the node with minimum weight and the number of iterations is bounded by N. To assign proper frequencies for anchors, the frequency assignment algorithm needs to go through all A anchors so its time complexity is $\mathcal{O}(A)$. For the route scheduling algorithm, if $k = m$, the time complexity is $\mathcal{O}(A^3 + N)$, i.e., Christofides $\mathcal{O}(A^3)$ algorithm [25] plus splitting demands over N. If $k > m$, the time complexity is $\mathcal{O}(A^3 + N + k + k\log k)$ which consists of a series computations in linear time and sorting operations. When A^3 is much larger than N and k, both cases have time complexity $\mathcal{O}(A^3)$ dominated by the Christofides algorithm.

6 Post-Optimization by Inserting Anchors

When node's battery deadline is not exceeded, there could be further room to optimize the results of the two-step algorithm. In this section, we propose a post-optimization algorithm. Since both objectives in Eq. (12) and Eq. (13) are the energy outputs from the SenCar's own battery, we can combine them into a single objective using the weighted method in [27], $F = w_1F_c + w_2F_m$.

The weights w_1 and w_2 are assigned by network administrators to measure the importance of energy charging cost compared to moving cost. If $w_2 > w_1$, it means that the administrator cares more about SenCar's moving cost over energy charging cost. For example, if $w_2/w_1 = 2$, for total cost F, reducing the moving cost by 1 J is equivalent to saving energy charging cost of 2 J on SenCars. In practice, we would expect $w_2 > w_1$ in most cases as the administrators want to minimize the recharge time by covering more nodes with anchors so a slight increase of energy cost due to multi-hop charging is acceptable.

6.1 Inserting Anchors

It is critical to observe that the optimal system cost F achieves a good compromise between F_c and F_m. In fact, any solution that can minimize F is said to be *Pareto optimal* when $w_1, w_2 \neq 0$ [28]. In multi-objective optimization, Pareto optimality describes a state that we cannot further increase the profit of one objective without reducing the profit of another objective. For our problem, it means that we cannot further reduce charging cost without increasing the moving cost on SenCars. On one hand, introducing more anchors would potentially increase SenCars' moving cost F_m; on the other hand, more anchors means fewer energy relays thus less energy charging cost F_c. Based on this observation, we propose a post-optimization algorithm that evaluates whether inserting an anchor into the established *charging sets* leads to lower system cost. However, since such insertion splits the original charging set, it would elongate the total recharge time of the route. To this end, the algorithm should also ensure anchor insertions do not cause battery depletion on subsequent nodes in the route. To keep it simple and effective in a dynamic network environment, we need to avoid computationally intensive algorithms.

The basic procedures is illustrated below. Initially, for each anchor a_i, a node with the maximum charging cost is selected in its charging set $\mathcal{S}_{a_i}$. Then these selected nodes are sorted in a descending order according to their charging costs.

The SenCar starts from the first node j in the list which has the maximum charging cost on the entire route. Tentatively designate node j as a new anchor because by charging j directly, a great amount of energy cost can be reduced. We denote node j as a new anchor a'_j. Next, an important step is to see whether we can further reduce energy charging cost by moving some of the elements from $\mathcal{S}_{a_i}$ to $\mathcal{S}_{a'_j}$.

This is because a node k in $\mathcal{S}_{a_i}$ may be more efficiently recharged via the new anchor. For each node k in $\mathcal{S}_{a_i}$, we compare if,

$$(1-\eta_{k,a_i})/\eta_{k,a_i} > (1-\eta_{k,a'_j})/\eta_{k,a'_j}. \tag{29}$$

If yes, we move node k to be covered in $\mathcal{S}_{a'_j}$ and denote the old a_i by a'_i after this operation. The new anchor will be assigned a new frequency band that is not being used by its neighbors. For k to join the new charging set, its resonant frequency is tuned to be the same as a'_j. All elements in $\mathcal{S}_{a_i}$ are examined to see whether it is beneficial to be included under the new anchor a'_j or remain with old anchor a_i. At this point, a new anchor a'_j is introduced to partition the original charging set whereas their joint coverage still remains the same.

6.2 Optimize Total Cost

The next step is to calculate whether there would be a reduction in the total cost F. Denote the changes of moving cost after introducing a'_j by ∂f_m and changes of charging cost by ∂f_c. We assume the new sequence $(a_1, a_2, \ldots, a'_i, a'_j, \ldots, a_{l_s})$ has the lowest moving cost so

$$\partial f_m = (c_{a_{i-1},a'_i} + c_{a'_i,a'_j} + c_{a'_j,a_{i+1}}) - (c_{a_{i-1},a_i} + c_{a_i,a_{i+1}}), \tag{30}$$

and

$$\partial f_c = \sum_{a\in\{a'_i,a'_j\}} \sum_{k\in\mathcal{S}_a} \frac{(1-\eta_{k,a})d_k}{\eta_{k,a}} - \sum_{k\in\mathcal{S}_{a_i}} \frac{(1-\eta_{k,a_i})d_k}{\eta_{k,a_i}}. \tag{31}$$

Then we see whether $\triangle F = w_1\partial f_c + w_2\partial f_m$ is less than zero. If yes, it means a reduction of F is accomplished.

6.3 Preserve Battery Deadline

Before the new anchor can be successfully added into the recharge route, the algorithm should check whether the insertion preserves time feasibility of the entire sequence. For the new sequence $(a_1, a_2, \ldots, a'_i, a'_j, \ldots, a_{l_s})$, a node with the minimum value of SenCar's arrival time minus lifetime is selected for each charging set ($\arg\max_{k\in\mathcal{S}_{a_i}}(A_k - L_k)$ for $A_k - L_k < 0$). The lifetime of this node represents the latest time for a SenCar to reach its superior anchor and the difference between A_k and L_k indicates the tightness of the battery deadline. The closer A_k approaches L_k, the less chance a new anchor can be inserted prior to this node without violating the battery deadline. Recall from Section 5.2.3 that the recharge time of a'_j's charging set $\mathcal{S}_{a'_j}$ is governed by the node with the maximum recharge time ($t_{a'_j} = \max_{i\in\mathcal{S}_{a'_j}} t_i$). Thus, the new insertion introduces an additional $\Delta T = t_{a'_j} + \partial f_m/v$ waiting time to all subsequent nodes after a'_j in the sequence. For anchor a_i from a'_j to a_{l_s}, the algorithm computes whether $A_{a_i} + \Delta T - L_{a_i} > 0$. If yes, it indicates the new anchor would potentially cause battery depletion in a_i's charging set and the insertion should be avoided. Otherwise, the new anchor can be successfully added into the recharge route and assigned an appropriate resonant frequency.

Algorithm 4. Post-optimization Algorithm for SenCar s

Input: Recharge sequence $a_1, a_2, \ldots, a_{l_s}$, set of anchors $\mathcal{A}_s$, energy demand d_i of node i, charging efficiency of j, $\eta_{j,i}$ if SenCar is at i, moving cost $c_{i,j}$ on edge (i,j), time feasibility mark at anchor $x \leftarrow 0$, objective weights w_1, w_2, charging set $\mathcal{S}_a$ for all anchors.
Output: A new recharge sequence consists of anchors.

$i \in \mathcal{S}_a$. Sort these nodes in descending order list $\mathcal{I}$. $j \leftarrow 1$.
while $x \neq a_{l_s}$ AND $\mathcal{I} \neq \emptyset$ **do**
  For $j > x$, consider j as a candidate anchor a'_j and $\forall k \in \mathcal{S}_{a_i}$.
  if $(1-\eta_{k,a_i})/\eta_{k,a_i} > (1-\eta_{k,a'_j})/\eta_{k,a'_j}$ **then**
    $\mathcal{S}_{a'_i} \leftarrow \mathcal{S}_{a_i} - k$, $\mathcal{S}_{a'_j} \leftarrow \mathcal{S}_{a'_j} + k$.
    $\partial f_m \leftarrow (c_{a_{i-1},a'_i} + c_{a'_i,a'_j} + c_{a'_j,a_{i+1}}) - (c_{a_{i-1},a_i} + c_{a_i,a_{i+1}})$.
    $\partial f_c \leftarrow \sum_{a\in\{a'_i,a'_j\}} \sum_{k\in\mathcal{S}_a} \frac{(1-\eta_{k,a})d_k}{\eta_{k,a}} - \sum_{k\in\mathcal{S}_{a_i}} \frac{(1-\eta_{k,a_i})d_k}{\eta_{k,a_i}}$.
    $\triangle F \leftarrow w_1\partial f_c + w_2\partial f_m$, new seq. $(a_1, \ldots, a'_i, a'_j, \ldots, a_{l_s})$.
    if $\triangle F < 0$ **then**
      For $A_k - L_k < 0$ in each charging set, find
      $k = \arg\max_{k\in\mathcal{S}_{a_i}}(A_k - L_k)$, $\Delta T = \max_{i\in\mathcal{S}_{a'_j}} t_i + \partial f_m/v$.
      for anchor a_i from a'_j to a_{l_s} **do**
        if $A_{a_i} + \Delta T - L_{a_i} > 0$ **then**
          When $a_i > x$, update mark $x \leftarrow a_i$,
          Declare time infeasible, **Break**.
        end if
      end for
      Insertion of a'_j is successful, $\mathcal{I} \leftarrow \mathcal{I} - j$, $j \leftarrow j+1$.
    else
      Consider next node j, $\mathcal{I} \leftarrow \mathcal{I} - j$, $j \leftarrow j+1$.
    end if
  end if
end while

To speed up the optimization process, whenever a new anchor insertion causes battery depletion at anchor a_i, a_i is marked, which means new anchors can only be inserted

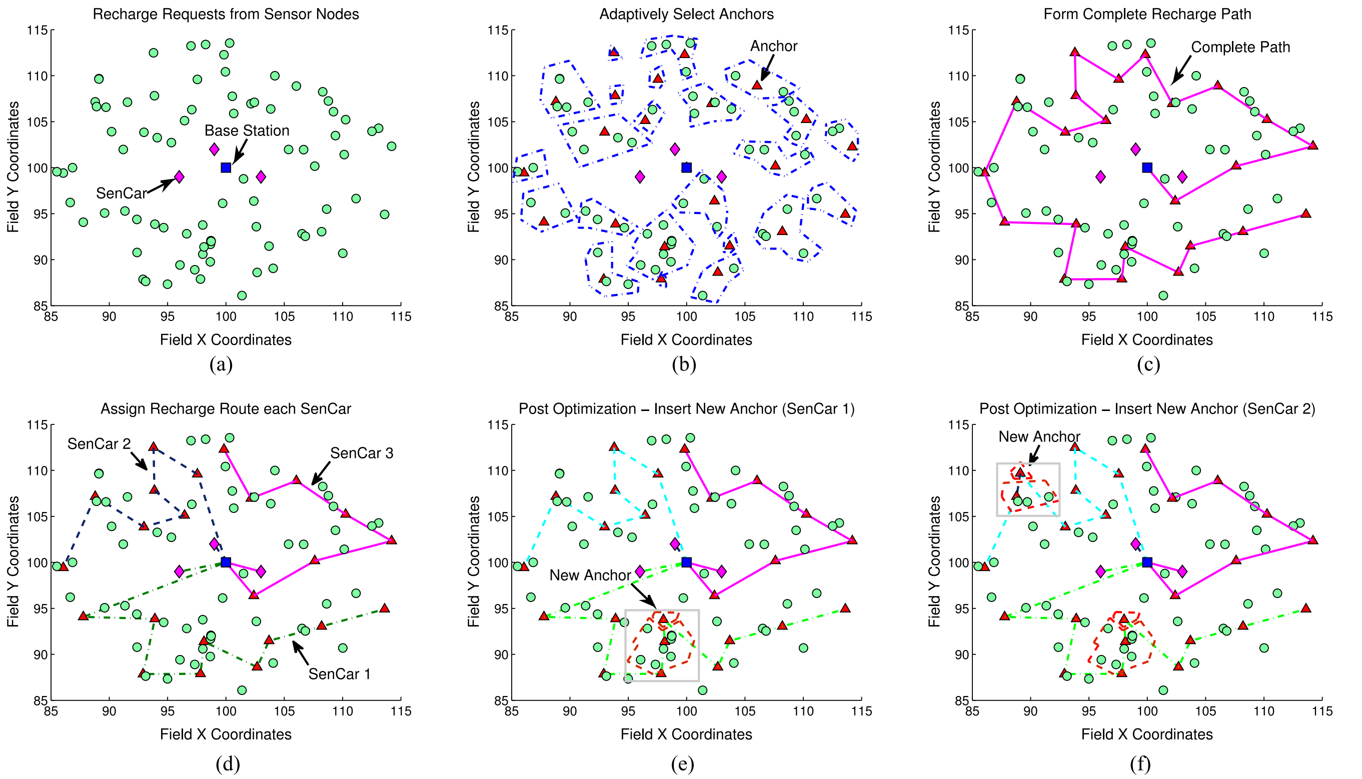

Fig. 5. A complete example of the algorithm. (a) SenCars receive a number of energy requests. (b) Find anchors among nodes. (c) Form a complete recharge path through anchors. (d) Assign recharge route to each SenCar. (e) Inserting an anchor in SenCar 1's route. (f) Inserting an anchor in SenCar 2's route.

after this location in the sequence. In the subsequent iterations, while a maximum charging cost node is being considered as a candidate anchor, the algorithm first checks its location with the previous mark. If its location is before the mark, the algorithm skips this node and proceeds to the next one. This operation saves a considerable amount of time by avoiding unnecessary computations that would lead to battery depletion ultimately. The algorithm terminates when a new anchor cannot be added into the recharge sequence, i.e., no more improvement on the system cost. The pseudo-code for the post-optimization algorithm is shown in Algorithm 4.

6.4 Time Complexity

We now analyze the time complexity of the algorithm. Since A anchors are generated from the two-step approximation algorithm, we need to check at most A charging sets. Suppose the size of maximum charging set is S_m. Initially, finding nodes with maximum charging cost for A anchors requires AS_m time and the sorting takes $A \log A$ time. In the worst case, the algorithm iterates through all A anchors and each iteration requires S_m for new anchor re-assignments and AS_m time for checking possible battery deadline violations. In sum, the post-optimization algorithm takes $\mathcal{O}(AS_m + A\log A + A(S_m + S_m A)) = \mathcal{O}(A^2 S_m + A(S_m + \log A))$.

Remarks: Although the proposed algorithms are centralized, they are implemented on the SenCars which have high-capacity batteries and orders of magnitude more computing, storage resources than the sensor nodes. In practice, we are currently implementing high-performance *Field-Programmable Gate Array* (FPGA) boards on the SenCars. For example, the latest Xilinx Virtex-7 FPGA contains 1.9 M logic cells, 3,600 digital signal processing slices and each one can operate at speed of 1.5 GHz[29]. Thus it is not difficult for them to handle computations for large networks.

6.5 A Complete Example

To see the entire operation of the algorithm more clearly, we show an example in Fig. 5. Fig. 5a demonstrates a snapshot during the operation of 3 SenCars ready to resolve 80 recharge requests of nodes with energy demands from 200-1,500 J. The first step is to find anchors that can offer entire coverage of all energy requests with the minimal charging cost. Fig. 5b shows the results of anchor selection algorithm. 23 anchors are selected and the largest charging set includes 9 nodes. For clarity, we only plot the charging set in Fig. 5b. In Fig. 5c, a complete recharge route is found through all the anchors starting from the base station using the Christofides algorithm [25]. In Fig. 5d, the complete recharge path is split into three different routes and each SenCar is assigned a route. Up to this point, SenCars can fulfill all the energy requests by stopping at anchor locations and charge nodes in multi-hops.

To further reduce the system cost, we conduct post-optimization procedures for each SenCar. For demonstration purposes, we use weights $w_1 = 1, w_2 = 3$ to evaluate the improvement by inserting an anchor and perform an iteration for all 3 SenCars. An anchor with maximum charging cost is selected in each route. We calculate the value of $\triangle F$ to see whether there is further saving in the system cost. Our algorithm yields $\triangle F_1 = -496$ J for SenCar 1, $\triangle F_2 = -490$ J for SenCar 2 and $\triangle F_3 = 130$ J for SenCar 3. The insertions would elongate durations of the three recharge routes by 68, 62 and 41 mins, respectively, which still satisfies the minimum battery deadline of the subsequent nodes. Since $\triangle F_1$, $\triangle F_2$ for SenCars 1 and 2 are less than zero, inserting

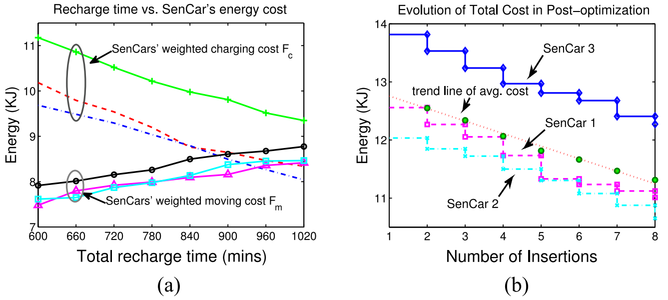

Fig. 6. Evaluation of algorithm design. (a) Relationships between energy cost and recharge time. (b) Effectiveness of post-optimization algorithm.

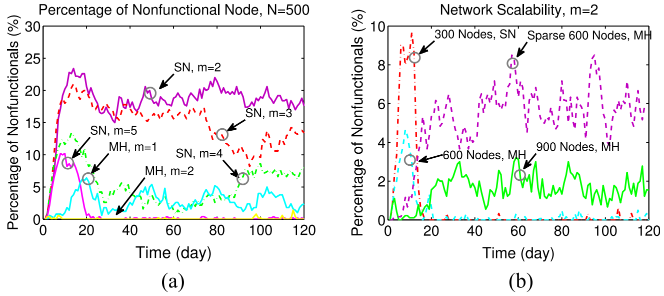

Fig. 7. Comparison on the number of nonfunctional nodes. (a) Performance comparison when $N = 500$. (b) Scalability evaluation when $m = 2$.

anchors at the locations shown in Fig. 5e has further reductions in system cost. On the other hand, since $\triangle F_3$ for SenCar 3 is larger than zero, there would be a slight increase of the total cost so we should not insert the anchor at the picked set. For clarity, we have shown two successful cases of anchor insertion in Fig. 5f for SenCars 1 and 2. The post-optimization process ends after each SenCar has examined all its charging sets for further improvement or a late recharge occurs.

7 Performance Evaluations

We have developed a discrete-event simulator to evaluate the performance of multi-hop wireless charging (denoted as "MH"). Since the works in [8], [9] do not provide concrete models of multi-hop wireless charging, it is very difficult to compare the performance with theirs. Actually, even the performance and cost of MH over the conventional single node wireless charging (denoted as "SN") is unknown. To this end, we decide to compare our framework with SN in [1], [2], [3], [4]. We distribute 500 sensor nodes uniformly randomly in a circular field with radius $R_c = 25$ m. The transmission distance and sensing range are $d_r = R_s = 5$ m. Sensors' energy consumptions are modeled according to [30]. By using some typical values of $e_0 = 50 \times 10^{-6}$ J/bit, $e_1 = 10 \times 10^{-7}$ J/bit, $\alpha = 4$ and $l_p = 32$ bits, e_c is 21 mJ for transmitting/receiving a packet. We set the total number of events $N_e = 5$ in each time slot and these events appear independently randomly from others at locations with probability $p = R_s^2/R_c^2 = 0.04$. The traffic rates for time-sensitive and time-insensitive packets are $\lambda_1 = \lambda_2 = 3$ pkt/min. We use Dijkstra's shortest path routing algorithm to direct packets to their destinations and set the data collection hop l to 2.

Recharge threshold β is critical to the overall performance. On one hand, if β is large, e.g., 90 percent, SenCar's recharge capacity may be easily overwhelmed upon receiving too many energy requests; on the other hand, if β is set to be very small, e.g., 10 percent, nodes might not have enough residual lifetime before the SenCar arrives, thereby causing large numbers of energy depletions. Therefore, we set β at 50 percent of the total battery capacity. We use an AAA NiMH battery of 780 mAh capacity working at 1.5 V. Recharge time is modeled from [19] with a maximum at 78 mins. The MH charging efficiency threshold is $\tau = 0.3$; any node with smaller charging efficiency will not receive any energy. All the SenCars and sensors have identical coils with $n_t = 300$ rounds and $r_s = 10$ cm. Wireless charging efficiencies are calculated using the procedures in Section 3.2. Each SenCar is equipped with a 12V battery[31]. At the speed of 1 m/s, the current draws from the battery is 4Ah. Thus, the moving energy consumption is $e_s = 48$ J/m. The simulation is set to run for 4 months' time.

7.1 Evaluation of Post-Optimization

First, we validate the designs of post-optimization algorithm. We evaluate the evolution of cost during the simulation when the energy requests are within the range of $[10, 120]$ with 3 SenCars. Fig. 6a shows the relation between recharge time and SenCar's energy cost. As we keep adding new anchors into the recharge route, the total recharge time increases from 600 to $1,020$ mins and the (weighted) moving costs F_m of SenCars also increase. On the other hand, energy charging cost F_c declines as more anchors are introduced into the routes. The evolution of SenCars' moving and charging costs validates that adding new anchors can reduce charging costs, elongate the recharge time span and increase SenCars' moving costs.

To visualize the progress of post-optimization more clearly, we trace the evolution of total energy cost on different SenCars and plot a trend line of their combined average cost in Fig. 6b. The x-axis represents the number of iterations before the algorithm terminates. We observe from the trend line that the post-optimization algorithm can effectively reduce the total energy cost by 12 percent. During simulations, once the algorithm detects an increase of total system cost after adding an anchor ($\triangle F > 0$), it removes the anchor from the route. New anchors are added when $\triangle F < 0$ and we observe that, on average, the post-optimization algorithm can effectively reduce total cost in each iteration in Fig. 6b. Thus the above results validate that the post-optimization algorithm further improves solutions.

7.2 Number of Nonfunctional Nodes

We now demonstrate the advantage of MH by comparing the number of nonfunctional nodes with SN. Once a node depletes its battery and no SenCar has arrived yet, it is nonfunctional until being recharged. Fig. 7a compares the number of nonfunctional nodes when $N = 500$. To keep nonfunctional nodes within 5 percent, at least 5 SenCars are needed for SN. In contrast, for MH, only 1 SenCar is needed and 2 SenCars can almost eliminate the chances of battery depletion over the entire operations. The surge of nonfunctional nodes around 10-15 days for SN is because the recharge requests have temporarily exceeded SenCars' capability. As the network reaches equilibrium, the curves decline gradually. However, this phenomenon does not appear in MH, which shows better robustness even with

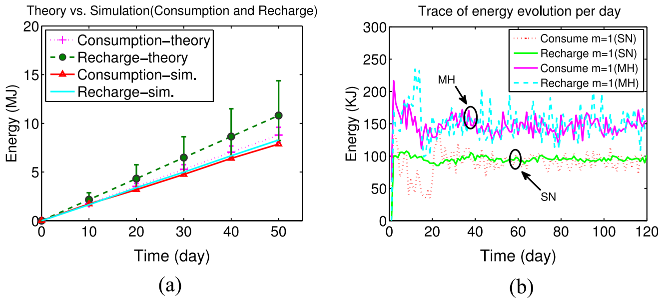

Fig. 8. Energy consumption versus replenishment $N = 500$. (a) Theoretical results versus simulations (MH, $m = 1$). (b) Trace of energy evolution for SN and MH ($m = 1$).

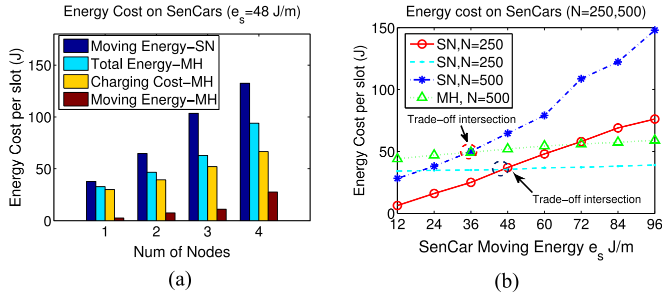

Fig. 9. Comparison of energy cost on SenCars to maintain nonfunctional nodes under 5 percent. (a) $e_s = 48$ J/m. (b) $e_s = 24$ to 96 J/m.

fewer SenCars. Recall from Eq. (9) that our calculation yields $m \geq 0.61$, which roughly matches our observation here that one SenCar can almost satisfy all the energy requests and two SenCars can maintain nonfunctional nodes close to zero.

To see the scalability improvement more clearly, we have conducted additional evaluation in Fig. 7b where we set $m = 2$ and $N = 300$ for SN to provide a baseline and increase N from 600 to 900 nodes. As we can see, the number of nonfunctional nodes still stays below 5 percent, which indicates a 3-fold increase in the nodes SenCars can cover compared to SN (900 nodes versus 300 nodes). In addition, we have also evaluated the performance of MH in sparse networks where node density is low. To maintain the connectivity among nodes, we double the radius of the field and fix N at 600 nodes. The node density diminishes 75 percent from 0.3 nodes/m^2 to 0.075 nodes/m^2. We observe that the number of nonfunctional nodes jumps slightly above 5 percent at equilibrium (not large). The results indicate that the advantage of MH could be weakened in a sparse network with lower node density. However, in the worst case, it is still equivalent to SN without any multi-hop energy relay.

7.3 Energy Consumption versus Replenishment

We now evaluate the amount of energy consumption and replenishment and validate the accuracies of our theoretical model. To better exhibit the gaps between curves, we plot the results for the first 50 days. Fig. 8a depicts energy consumption and replenishment curves for the theoretical and simulation results of MH, $m = 1$. For the theoretical consumption curve, we delineate the mean values with ranges representing standard deviations from the means. For the theoretical replenishment curve, we use the average charging rate for the battery in [19] as a base and the maximum and minimum rates are indicated by the range of the curve. First, we observe that the replenishment curve is above the energy consumption curve for both theoretical and simulation results. This indicates that SenCars can put more energy back into the network than consumed, which is consistent with our observations in Fig. 7a (that is, almost all the nodes are functional). Our theoretical analysis on the energy consumptions can achieve very high estimation accuracy, as indicated by the small gap between the two curves. The gap between replenishment curves is wider, which is due to the idle time between two successive recharge operations. When the number of SenCars is sufficient, the recharge requests are sparse over time and SenCars do not need to perform recharge continuously, thus the gap is in between.

We also trace the energy evolution of energy consumption and replenishment in Fig. 8b. For SN, the energy consumption curve quickly drops from the very beginning until it hits a bottom around 20 days. As the SenCar slowly resolves nonfunctional nodes, these nodes resume normal operation (consume energy) which corresponds to the jump-up of the energy consumption curve at 20 days and the two curves enter an equilibrium after 40 days. On the other hand, for MH, a large gap is observed from SN, indicating 50 percent more energy being replenished into the network. The improved recharge capability is clearly observed during the first 20 days. That is, in contrast to the slow response in SN, the replenishment curve of MH surges when the energy consumption curve has a sharp decline. It means that whenever nodes are becoming nonfunctional and stop consuming energy, they are quickly recharged by the SenCar.

7.4 System Energy Cost

We now compare the energy cost of MH and SN and explore possible trade-offs between the two schemes. In Fig. 9, we evaluate the energy cost needed to maintain the same quality of service (nonfunctional $<$ 5 percent). In Fig. 9a, for MH, we show energy costs from both node recharging and SenCar movement, as well as the sum of them and compare with the total cost of SN, while varying N from 250-1,000. When $N = 250$, the total cost is almost equivalent while increasing N results in better efficiency for MH. This is because that when node density is higher, more nodes can be recharged simultaneously without the hassle of approaching them one by one. If multi-hop charging cost is much less than moving cost e_s, it is more cost-effective to use MH.

To visualize the trade-offs between MH and SN, we adjust the moving cost e_s from 12 to 96 J/m in Fig. 9b which represents different energy efficiencies of the SenCar's battery and motors. For $N = 250$, a trade-off point around 46 J/m is observed. When $e_s < 46$ J/m, SN is more cost-effective. A similar result is observed for $N = 500$ where the trade-off point is around 36 J/m. These results indicate that if energy charging cost can be compensated by shorter moving distances, MH would have less total cost. Based on these results, the network administrator can decide which scheme to use given the system parameters.

7.5 Trade-Offs Between Charging and Moving Costs

In this section, we further explore the subtle relations between the two optimization objectives by finding pareto

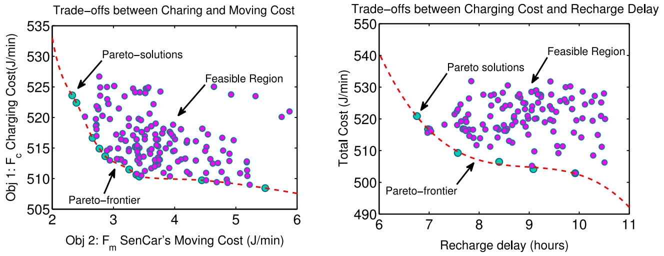

(a) (b)

Fig. 10. Evaluation of trade-offs in the network. (a) Trade-offs between SenCar's charging and moving costs. (b) Trade-offs between total system cost and recharge delay.

solutions generated by the algorithm. Note that since the problem is NP-hard and intractable in polynomial time, the pareto solutions found by the algorithm are in fact sub-optimal and within the approximation bounds discussed in Section 5.3. As shown in [28], a minimizer of the weighted combination of objectives in Eqs. (12) and (13) is a pareto optimal solution to the original bi-objective problem in Eq. (11). To explore the solution space, we vary the weights w_1 and w_2 from 1 to 10 in small increments and delineate those solutions of SenCars' charging cost and moving cost in Fig. 10a. The y-axis represents SenCar's charging cost F_c (the first objective) and the x-axis represents SenCar's moving cost F_m (the second objective). In the post-optimization algorithm, the choice of different weights allows the SenCar to explore different solutions and it has a direct impact on the decision value $\triangle F$ as well as the recharge routes. From Fig. 10a, we can see that the points along the *pareto-frontier* form a contour to bound the feasible solution space. The *pareto-frontier* consists of solutions that cannot be surpassed by any other alternative solutions. As analyzed in our algorithm designs, a trade-off is observed between the two optimization objectives. That is, when the SenCar's moving cost is reduced, the charging cost has to increase and vice versa.

Similarly, we also examine the trade-offs between the total system cost and recharge delay. As shown in Fig. 10b, if we want to reduce system cost, a certain amount of nodes would suffer from extended recharge delay. These results validate our designs and analysis in the algorithm as we aim to reduce system cost as much as possible while minimizing the chances of battery depletion.

7.6 Evaluation of Network Delay

For successful and timely packet delivery, all the nodes on the routing paths should be functional. If a node becomes nonfunctional on a routing path and there is no alternative path, its upstream node buffers packets until the routing path is recovered by SenCars. Table 3 reports average latencies for both time-sensitive (TS) and time-insensitive (TI) packets. We can see that MH has much shorter latency than SN for both TS and TI packets because of much lower fractions of nonfunctional nodes during the operations. Once packets are generated, they can be immediately routed to the destination with less chance of experiencing buffering delays. To check with the upper bound for time-insensitive packets in Eq. (10), we plug the corresponding system parameters into the equation and obtain $T_d < 21$ hours. Accordingly, our simulation results show the longest network delay of time-insensitive packets is 660 mins (11 hours) which is 52 percent of the upper bound.

TABLE 3
Average Packet Latencies (Mins)

	TS(SN)	TI(SN)	TS(MH)	TI(MH)
$m=1$	698	660	8.98	497
$m=2$	549	374	8.83	278
$m=3$	393	289	7.97	187
$m=4$	259	267	7.82	138
$m=5$	163	249	7.68	125

7.7 Evaluation of Recharge Delay and Service Interruptions

Since some nodes may have similar energy consumption rates, it is possible for them to request recharge at the same time. If the requests are scattered at different locations, due to limited multi-hop charging range, the SenCar may not be able to cover all the requests at once. In this case, late recharge is inevitable and its duration is measured by recharge delay. Fig. 11 compares recharge delay of SN and MH. Recall from Section 7.2 that for $N=500$, SN $m=5$ and MH $m=2$ have comparable nonfunctional percentage under 5 percent. For SN, Fig. 11a shows that some nodes would experience more than 50 hours of recharge delay. In other words, it means that once a node has requested for recharge, there are at least 50 nodes in SenCars' service queues ahead of this node waiting for recharge. In contrast, Fig. 11b presents much better results with MH while the number of SenCars is only $m=2$. We can see that a majority (almost 80 percent) of nodes have even no recharge delay and very few nodes have recharge delay over 20 hours. The huge improvements are due to extended charging range which upgrades the single-server queue of SN into a multi-server queue in MH. The SenCars have extra capabilities to handle energy requests in the vicinity thereby expediting the entire recharging process.

We also present the percentage of nonfunctional durations in a geographical view in Fig. 12 where x and y axes are field coordinates. The time duration while a node is in nonfunctional status greatly impacts the network operation. Such nodes are not able to sense the environment and may miss important events, constituting service interruptions. For fair comparison, we set $N=500$ and $m=2$ for both cases. SN results in a maximum of 75 percent time in nonfunctional status with the average over 40 percent widely spreading on the entire field. In sharp contrast, MH has the

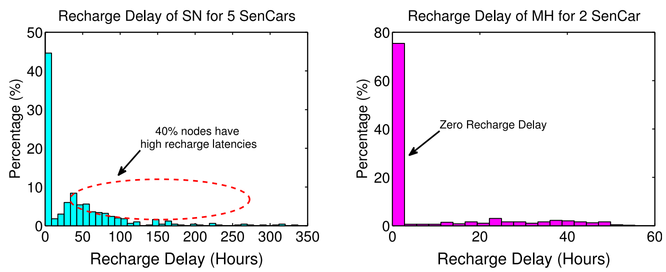

(a) (b)

Fig. 11. Comparison of recharge delay when SN and MH have similar nonfunctional percentage. (a) SN, $m=5$. (b) MH, $m=2$.

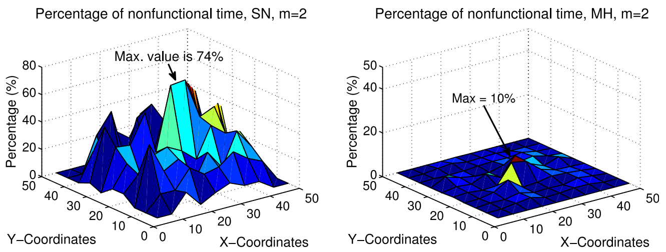

(a) (b)

Fig. 12. Comparison of nonfunctional nodes' durations $N = 500, m = 2$. (a) SN. (b) MH.

maximum of only 10 percent with an average below 3 percent. This shows that MH has significantly less service interruptions than SN.

8 Discussions

In practice, the effectiveness of multi-hop wireless charging could be affected by node density and topology. For sparse networks, it is possible that a node has no immediate neighbors to relay energy. In this case, our scheme still works, but reduces to a single node recharge method. In fact, due to the declining manufacturing cost of sensor nodes, and the needs to ensure robustness against node and communication failures and faults, they are usually deployed at densities much higher than needed for monitoring. Some applications even require k-coverage, where each point on the field is monitored by at least k sensors. For example, to detect forest fires, different parameters across multi-dimensions are collected to create a potential ignition map of the forest. For better reliability, indicator for each location is usually calculated based on the readings from multiple sensors. High density is desired for load balancing purposes as well. For example, nodes have higher densities near the sink so they can take turns forwarding data to extend network lifetime and improve robustness. Such high density deployment presents opportunities to apply our multi-hop recharging method. In reality, multi-hop wireless charging can make use of this node redundancy to improve network lifetime.

Another practical challenge is that the node topology may cause misalignment of sensor coils and degrade charging efficiency. Fortunately, recent research using coil arrays provides position-free solutions to the misalignment problem and it is found that charging efficiency increases from 4.8 to 64 percent [32]. Another option is to use mechanisms similar to "sliding antennas" [33] to fine tune and align the orientations of coils on demand.

The past several years have witnessed the rapid advance and maturity of wireless charging technology. One prominent example among others is *WiTricity*, a major player in the wireless charging market. It has recently released multiple products for consumer electronics, automobiles, medical and industrial applications. Its research and standardization efforts in wireless repeaters have effectively increased charging distance, scale and efficiency [34]. Our paper works in the same principle of resonant repeaters, which can be embedded under the floor, table or even walls to hop power in a room. Besides, researchers have accomplished a new milestone to extend charging distance significantly. They invented the *Dipole Coil Resonant System* based on refined coil structures that can power 40 smartphones from 5 meters and a single device from 9 meters[35] (close to sensors' transmission range). Combined with resonant repeaters for energy relay, energy delivery over multiple hops as studied in our framework is not only feasible in principle, but could soon be implemented based on all these recent technology advances.

9 Conclusion

In this paper, we employ resonant repeaters to improve the efficiency and scalability of recharge in WRSNs. We present detailed procedures to calculate multi-hop wireless charging efficiency based on the laws in physics and electronics that have been overlooked by previous studies. We introduce a hybrid data collection strategy to achieve a balance between routing cost and data latency, and establish a mathematical model to estimate scalability improvement and the number of SenCars required. We formulate the recharge scheduling problem into a multi-objective optimization problem, which is NP-hard. To achieve low-complexity, we propose a two-step approximation algorithm with bounded ratio for each objective followed by a post-optimization algorithm to further reduce the system cost. Finally, we evaluate the proposed framework by extensive simulations and compare with previous works. The results reveal much better network scalability and performance of our algorithm, and also validate our theoretical analysis.

Acknowledgments

The work in this paper was supported in part by the grant from US National Science Foundation under grant number ECCS-1307576.

References

[1] B. Tong, Z. Li, G. Wang, and W. Zhang, "How wireless power charging technology affects sensor network deployment and routing," in *Proc. 30th IEEE Int. Conf. Distrib. Comput. Syst. Workshops*, 2010, pp. 438–447.

[2] Y. Peng, Z. Li, W. Zhang, and D. Qiao, "Prolonging sensor network lifetime through wireless charging," in *Proc. IEEE 31st Real-Time Syst. Symp.*, 2010, pp. 129–139.

[3] Y. Shi, L. Xie, T. Hou, and H. Sherali, "On renewable sensor networks with wireless energy transfer," in *Proc. IEEE INFOCOM*, 2011, pp. 1350–1358.

[4] C. Wang, J. Li, F. Ye and, Y. Yang, "NETWRAP: An NDN based real-time wireless recharging framework for wireless sensor networks," *IEEE Trans. Mobile Comput*, vol. 13, no. 6, pp. 1283-1297, Jun. 2014.

[5] M. Watfa, H. AlHassanieh, and S. Selman, "Multi-hop wireless energy transfer in WSNs," *IEEE Commun. Lett.*, vol. 15, no. 12, pp. 1275–1277, Dec. 2011.

[6] M. Ma and Y. Yang, "SenCar: An energy efficient data gathering mechanism for large scale multihop sensor networks," *IEEE Trans. Parallel Distrib. Sys.*, vol. 18, no. 10, pp. 1476–1488, Oct. 2007.

[7] M. Zhao, Y. Yang, and C. Wang, "Mobile data gathering with load balanced clustering and dual data uploading in wireless sensor networks," *IEEE Trans. Mobile Comput.*, vol. 14, no. 4, pp. 1536–1233, Mar. 2015.

[8] X. Liu, J. Luo, K. Han, and G. Shi, "Fueling wireless networks perpetually: A case of multi-hop wireless power distribution," in *Proc. IEEE 24th Int. Symp. Personal, Indoor Mobile Radio Commun.*, 2013, pp. 1994–1999.

[9] L. Xie, Y. Shi, T. Hou, W. Lou, H. Sherali, and S. Midkiff, "On the renewable sensor networks with wireless energy transfer: The multi-node case," *Proc. 9th Annu. Conf. Sensor, Mesh Ad Hoc Commun. Netw.*, 2012, pp. 10–18.

[10] S. Guo, C. Wang, and Y. Yang, "Joint mobile data gathering and energy provisioning in wireless rechargeable sensor networks," *IEEE Trans. Mobile Comput.*, vol. 13, no. 12, pp. 2836–2852, Dec. 2014.

[11] M. Zhao, J. Li, and Y. Yang, "A framework of joint mobile energy replenishment and data gathering in wireless rechargeable sensor networks," *IEEE Trans. Mobile Comput.*, vol. 13, no. 12, pp. 2689–2705, Dec. 2014.

[12] M. Zhao and Y. Yang, "Optimization-based distributed algorithms for mobile data gathering in wireless sensor networks," *IEEE Trans. Mobile Comput.*, vol. 11, no. 10, pp. 1464–1477, Oct. 2012.

[13] F. Zhang, S. Hackworth, W. Fu, and M. Sun, "The relay effect on wireless power transfer using witricity," in *IEEE 14th Conf. Electromagn. Field Comput.*, 2010, p. 1.

[14] B. Lee, A. Hillenius, and D. Ricketts, "Magnetic resonant wireless power delivery for distrbuted sensor and wireless systems," in *Proc. IEEE Topical Conf. Wireless Sensors Sensor Netw.*, 2012, pp. 13–16.

[15] C. Wang, J. Li, F. Ye, and Y. Yang, "Recharging schedules for wireless sensor networks with vehicle movement costs and capacity constraints," in *Proc. 11th Annu. IEEE Int. Conf. Sensing Commun. Netw.*, 2014, pp. 468–476.

[16] W. Zhong, C. Lee, and S. Hui, "Wireless power domino-resonator systems with noncoaxial axes and circular structures," *IEEE Trans. Power Electron.*, vol. 27, no. 11, pp. 4750–4762, Nov. 2012.

[17] J.O. Mur-Miranda, et al., "Wireless power transfer using weakly coupled magnetostatic resonators," in *Proc. IEEE Energy Convers. Congr. Expo.*, 2010, pp. 4179–4186.

[18] Price of Copper Tube. (2016). [Online]. Available: http://coppertubingsales.com/copper-coils/copper-coils-standard/typel-copper-coil-astm

[19] (2016). *Panasonic Ni-MH battery handbook*, [Online]. Available: http://www2.renovaar.ee/userfiles/Panasonic_Ni-MH_Handbook.pdf

[20] G. Nagy and S. Salhi, "Location-routing: issues, models and methods," *Eur. J. Oper. Res.*, vol. 177, pp. 649–672, 2007.

[21] B. Gavish, "A note on the formulation of the m-salesman traveling salesman problem," *Manag. Sci.*, vol. 22, pp. 704–705, 1976.

[22] R. M. Karp, "Reducibility Among Combinatorial Problems," New York, NY, USA: Springer, 1973, pp. 85–103.

[23] D. Zuckerman, "Linear degree extractors and the inapproximability of max clique and chromatic number," in *Proc. ACM Symp. Theory Comput.*, 2006, pp. 681–690.

[24] G. Frederickson, M. Hecht, and C. Kim, "Approximation algorithms for some routing problems," *SIAM J. Comput.*, vol. 7, no. 2, pp. 178–193, 1978.

[25] N. Christofides, "Worst-case analysis of a new heuristic for the travelling salesman problem," Carnegie Mellon Univ., Pittsburgh, PA, USA, Tech. Rep. 388, 1976.

[26] C. Lund and M. Yannakakis, "On the hardness of approximating minimization problems," *J. ACM*, vol. 41, no. 5, pp. 960-981, 1994.

[27] T. Marler and J. Arora, "The weighted sum method for multi-objective optimization: new insights," *Struct. Multidiscip. Optim.*, vol. 41, no. 6, pp 853–862, Jun. 2010.

[28] F. Szidarovszky, M. Gerson, and L. Duckstein *Techniques for Multi-Objective Decision Making in Systems Management*. New York, NY, USA: Elsevier, 1986.

[29] (2016). *Xilinx Virtex-7*, [Online]. Avaiable: http://www.xilinx.com/products/silicon-devices/fpga/virtex-7.html

[30] W. R. Heinzelman, A. Chandrakasan, and H. Balakrishnan, "Energy-efficient communication protocol for wireless microsensor networks," in *Proc. 33rd Annu. Hawaii Int. Conf. Syst. Sci.*, 2000, p. 8020.

[31] (2016). SenCar's battery pack. [Online]. Avaiable: http://www.batteryclerk.com/store/p/63932-AJC-12V-4Ah-Sealed-Lead-Acid-AGM-VRLA-Battery.html

[32] K. Mori, H. Lim, S. Iguchi, K. Ishida, M. Takamiya, and T. Sakurai, "Positioning-free resonant wireless power transmission sheet with staggered repeater coil array (SRCA)," *IEEE Antennas Wirel. Propag. Lett.*, vol. 11, no. 1, pp. 1710–1713, Dec. 2012.

[33] F. Adib, S. Kumar, O. Aryan, S. Gollakota, and D. Katabi, "Interference alignment by motion," in *Proc. 19th Annu. Int. Conf. Mobile Comput. Netw.*, 2013, pp. 279–290.

[34] (2014). *The next generation of wireless power*, [Online]. Available: http://witricity.com/assets/witricity_infographic_r13_small.pdf

[35] (2014). *Dipole Coil Resonant System*, [Online]. Available: http://www.gizmag.com/kaist-dipole-coil-resonant-system-wireless-charging/31876

[36] Y. Yang and C. Wang, *Wireless Rechargeable Sensor Networks*, Springer, 2015.

[37] M. Zhao, D. Gong, and Y. Yang, "Network cost minimization for mobile data gathering in wireless sensor networks," *IEEE Trans. Commun.*, vol. 63, no. 11, pp. 4418–4432, 2015.

[38] M. Ma and Y. Yang, "Clustering and load balancing in hybrid sensor networks with mobile cluster heads," *3rd Int. Conf. Quality Service. Heterogeneous Wired/wireless Netw.*, 2006.

Cong Wang received the BEng degree in information engineering from the Chinese University of Hong Kong and MS degree in electrical engineering from Columbia University, New York. He is currently working towards the PhD degree in the Department of Electrical and Computer Engineering, Stony Brook University, New York. His research interests include wireless sensor networks, performance evaluation of network protocols, and algorithms.

Ji Li received the BS degree in electrical engineering from Harbin Engineering University, Harbin, China, and the MS degree in electrical engineering from Zhejiang University, Hangzhou, China. He is currently working toward the PhD degree in the Department of Electrical and Computer Engineering, Stony Brook University, Stony Brook, New York. His research interests include wireless sensor networks and embedded systems.

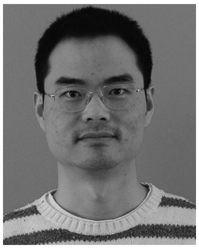

Fan Ye received the BE and MS degrees from Tsinghua University. He received the PhD degree from the Computer Science Department, University of California, Los Angeles. He is an assistant professor in the ECE Department at Stony Brook University. He has published more than 60 peer reviewed papers that have received more than 7,000 citations according to Google Scholar. He has 21 granted/pending US and international patents/applications. He was the co-chair for the Mobile Computing Professional Interests Community at IBM Watson for two years. He received the IBM Research Division Award, 5 Invention Achievement Plateau awards, and the Best Paper Award for International Conference on Parallel Computing 2008. His current research interests include mobile sensing platforms, systems and applications, Internet-of-Things, indoor location sensing, and wireless and sensor networks.

Yuanyuan Yang received the BEng and MS degrees in computer science and engineering from Tsinghua University, Beijing, China, and the MSE and PhD degrees in computer science from Johns Hopkins University, Baltimore, Maryland. She is a professor of computer engineering and computer science at Stony Brook University, New York. Her research interests include wireless networks, data center networks, optical networks and high-speed networks. She has published more than 340 papers in major journals and refereed conference proceedings and holds seven US patents in these areas. She is currently the associate editor-in-chief for the *IEEE Transactions on Cloud Computing* and an associate editor for the *Journal of Parallel and Distributed Computing*. She has served as the associate editor-in-chief for the *IEEE Transactions on Computers* and an associate editor for the *IEEE Transactions on Computers and IEEE Transactions on Parallel and Distributed Systems*. She has served as a general chair, program chair, or vice chair for several major conferences and a program committee member for numerous conferences. She is a fellow of the IEEE.